Dynamin: Regulation of Vesicle Cycling and Resting Stability of Vesicles at Presynaptic Terminals

BY

ANDREW BURGESS SEYMOUR
B.S., Carnegie Mellon University, 1997
M.S., Loyola University Chicago, 2005

THESIS

Submitted as partial fulfillment of the requirements
for the degree of Doctor of Philosophy in Biological Sciences
in the Graduate College of the
University of Illinois at Chicago, 2013

Chicago, Illinois

Defense Committee:

Janet Richmond, Chair, Biological Sciences
Simon Alford, Advisor, Biological Sciences
David Featherstone, Biological Sciences
Robert Paul Malchow, Biological Sciences
John Larson, Psychiatry

DYNAMIN: REGULATION OF VESICLE CYCLING AND RESTING STABILITY OF VESICLES AT PRESYNAPTIC TERMINALS

Andrew Burgess Seymour, Ph.D.
Neurobiology Program
Department of Biological Sciences
University of Illinois at Chicago
Chicago, Illinois (2013)

Dissertation Chairperson: Janet Richmond, PhD

Compensatory synaptic vesicle endocytosis during kiss-and-run vesicle fusion is not fully understood. Specifically, it is unclear whether proteins involved in classical clathrin-mediated endocytosis (CME) are also required for vesicle retrieval following kiss-and-run vesicle fusion. Part of the impetus for the work presented in this thesis was to determine whether one such protein, dynamin, is responsible for vesicle retrieval during kiss-and-run fusion. Dynamin is a key protein in membrane fission during CME, providing an energy utilizing GTPase reaction to sever the vesicle from the plasma membrane. However, because vesicles may not fully collapse during kiss-and-run fusion it is unclear whether there exists an analogous role for dynamin in this process. Utilizing a 5-HT-mediated model of presynaptic inhibition favoring kiss-and-run vesicle fusion in a model synapse, the lamprey giant reticulospinal synapse, I present findings that demonstrate kiss-and-run fusion as a frequency-dependent, calcium-sensitive effect of 5-HT. Furthermore, I demonstrate that dynamin does not appear to be conclusively involved in compensatory endocytosis during kiss-and-run vesicle fusion. While addressing this question, I employed different means of pharmacologically inhibiting dynamin. These experiments revealed that inhibition

of the action of dynamin, either by inactivating its GTPase activity, or by modifying its interaction with amphiphysin, depletes synaptic vesicle numbers at presynaptic active zones. This finding suggests that dynamin is important in maintaining vesicle pools in resting presynaptic terminals, but also provides new avenues for better elucidating potential roles of endocytic proteins in paradigms used to investigate kiss-and-run vesicle fusion.

These pages are dedicated to the individuals who have supported me in my endeavors and helped shape me into the person I am today: my mother – Dianne Seymour, my father – James Seymour, my sister – Molly Ghahtani, and my wife, Lakeisha Seymour. I appreciate all the sacrifices you have made to allow me to reach my potential, as well as the values you have instilled in me regarding my intellectual, creative, and professional pursuits.

Acknowledgement

I express sincerest gratitude to my advisor Dr. Simon Alford, who took me under his wing and gave me the freedom to grow through painstaking trial and error into a confident scientist. His generous devotion of time and energy, coupled with his endless patience and impressive wealth of knowledge gave me an opportunity to grow and learn in an exciting, supportive environment. I also want to acknowledge my committee, including Dr. Janet Richmond, Dr. David Featherstone, Dr. Paul Malchow, and Dr. John Larson, who gave me compassionate encouragement and critical feedback that allowed me to push myself to see farther than I could have without them. My experience at University of Illinois at Chicago would not have been complete without the encouragement and friendships I shared with so many wonderful people in the Alford laboratory, including Dr. Simon Alford, Dr. Edaeni Hamid, Michael Alpert, Shankar Ramachandran, Emily Church, Dr. Roy Smetana, Adam Bleckert, and Dr. Brian Page. Our discussions ranged from science to religion to food to music. Even without windows in our growing laboratory, you managed to shed light on so much and make it worthwhile, even when it didn't seem so. Dr. Thomas Park and Dr. A. Don Murphy deserve special thanks for providing me professional wisdom and kindheartedness when I needed it most. I thank my best friends Dr. Jason Herrick and Michael Massie for their unwavering love and empathy during my professional growth at UIC. I thank my parents and all of my family, whose

support was instrumental in my success. Finally, I thank my wife and children, without whom, I would not be here today.

TABLE OF CONTENTS

TABLE OF CONTENTS (continued)

LIST OF FIGURES

LIST OF FIGURES (continued)

LIST OF ABBREVIATIONS

5-HT	5-Hydroxytryptamine
BoNT	Botulinum neurotoxin
Ca^{2+}	Calcium ion
CNS	Central nervous system
DIP	Dynamin inhibitory peptide
DMSO	Dimethyl sulfoxide
EGTA	Ethylene glycol tetraacetic acid
EPSC	Excitatory postsynaptic current
GPCRs	G-protein coupled receptors
R	Receptor
SNAP-25	Synaptosomal-associated protein of 25 KDa
SNARE	Soluble-N-ethylmaleimide-sensitive factor attachment protein receptor
Syt	Synaptotagmin
TTX	Tetrodotoxin

1. INTRODUCTION

1.1 Players in Vesicle Fusion

Vesicle fusion during neurotransmitter release involves a coordinated interaction of many proteins. These proteins serve to bring vesicles in close proximity to the presynaptic membrane. Synaptic plasticity, one of the many ways in which the nervous system modifies the strength of its interacting neurons to respond to a changing environment, is thought to be conferred via modification of a variety of these proteins. These proteins are expressed in both the target/presynaptic membrane and the vesicle membrane, and together comprise the soluble-N-ethylmaleimide-sensitive factor attachment protein receptor (SNARE) complex (Schiavo et al., 1997; Rickman et al., 2004). The SNARE proteins are critical for fusion during the last step in neurotransmitter release following vesicle priming. Synaptobrevin/vesicle associated membrane protein (VAMP) is the major synaptic vesicle associated SNARE (Deak et al., 2004), whereas syntaxin (Hammarlund et al., 2007) and synaptosomal-associated protein of 25 kDa (SNAP-25) (Mehta et al., 1996) are associated within a specialized area of the target/presynaptic membrane in which vesicle fusion has been shown to occur, known as “the active zone”. These proteins are believed to play a critical role in neuronal communication, considering that mutations of these proteins has been shown to inhibit neurotransmission (Broadie et al., 1995; Deitcher et al., 1998; Littleton et al., 1998). In addition, clostridial toxins are known to severely impair the release of neurotransmitter through cleavage of individual SNARE proteins prior to formation of the core complex following

priming (Hayashi et al., 1994; Gerachshenko et al., 2005). For instance, botulinum neurotoxin B light chain potently inhibits neurotransmission in paired recordings, but only after a readily releasable, that is, primed, pool of vesicles is depleted by a stimulation train (Gerachshenko et al., 2005).

1.2 G-protein-coupled receptor mediated presynaptic inhibition

There is a vast literature describing neurotransmitter release in terms of vesicular quanta (del Castillo and Katz, 1954; Heuser et al., 1979), which describes all vesicles containing equal amounts of transmitter fusing and releasing their entire contents in the synaptic cleft at fixed rates. However, transient fusion events, colloquially known as kiss-and-run fusion, which alter neurotransmitter release, have been shown (Schneider, 2001; Palfrey and Artalejo, 2003; Aravanis et al., 2003a; Wightman and Haynes, 2004; Zefirov et al., 2004; Chen et al., 2005b; Harata et al., 2006a; Gerachshenko et al., 2009a; Takei et al., 2012). In the lamprey giant reticulospinal axons, activation of a presynaptic 5-hydroxytryptamine G protein-coupled receptor (GPCR) nearly abolishes glutamate release (Buchanan and Grillner, 1991), and does so independently of presynaptic calcium (Blackmer et al., 2001; Takahashi et al., 2001). While calcium channel independent modulation by GPCRs has been shown at the neuromuscular junction (Silinsky, 1984) and other synapses (Nurrish et al., 1999; Sakaba and Neher, 2003; Harvey and Stephens, 2004), GPCR-mediated presynaptic inhibition is widespread. While the underlying mechanisms remain to be fully elucidated, evidence has accumulated suggesting

a mechanism by which GPCR-mediated presynaptic inhibition occurs. For instance, in the lamprey giant reticulospinal synapse, 5-HT-mediated inhibition of neurotransmitter release is mediated by Gβγ (Blackmer et al., 2001; Takahashi et al., 2001), a downstream effector of a receptor found in the lamprey that is functionally similar to the 5-HT1b/1d receptor; this effector binds to SNAP-25 in SNARE complexes (Gerachshenko et al., 2005). Furthermore, synaptic vesicles are known to partially fuse with the presynaptic terminal (Ceccarelli et al., 1973; Klyachko and Jackson, 2002; Choi et al., 2003; Gandhi and Stevens, 2003; Pawlu et al., 2004; Photowala et al., 2006), as shown with FM dye fluorescence measurements. Similarly, kiss-and-run events have also been observed in neuroendocrine cells, where large dense-core vesicles, transiently fuse, with the membrane (Artalejo et al., 1998a) varying release (Graham et al., 2000; Elhamdani et al., 2001), potentially via Gβγ (Chen et al., 2005c). While FM dye fluorescence measurements demonstrate that vesicles transiently fusing with the presynaptic membrane are subsequently retrieved without complete loss of fluorescent labeled lipid (Kavalali et al., 1999; Pyle et al., 2000; Zakharenko et al., 2002; Aravanis et al., 2003b; Chen et al., 2004a), quenching of the fluorescence is possible via sulforhodamine, a water-soluble membrane impermeant fluorophore (Photowala et al., 2006). This demonstrates that the vesicles fusing via kiss-and-run actually contact the extracellular space during inhibition of synaptic transmission via 5-HT. Considerable evidence for a G-protein-coupled receptor-based model of presynaptic plasticity has been generated that explains changes in vesicle fusion as a result of a downstream

effector of the 5-HT1b/1d receptor (Blackmer et al., 2005; Gerachshenko et al., 2005; Schwartz et al., 2007; Yoon et al., 2007a).

Serotonin, a relatively well-known neurotransmitter, has a reputation that seems out of step with its availability in the CNS, considering that approximately 90% of the body's serotonin is outside the CNS, within enterochromaffin cells in the intestinal lumen; additionally, serotonin also plays a role in vascular constriction (Artalejo et al., 1998b; Yao et al., 2006; Harata et al., 2006a). Nonetheless, serotonin's effects in the CNS are numerous, including, but not limited to, regulation of mood and appetite, anxiety, and learning and memory. As such, it has been an actively targeted neurotransmitter for neuroscience, pharmacology, medicine, psychiatry, and a host of other disciplines aimed at improvements in understanding human health and interventions for various debilitating diseases.

Within the CNS of jawed vertebrates (from bony fishes to mammals), serotonin is produced in hindbrain as part of the raphe nuclei, which appears as a ridge of cells in the center and most medial portion of the reticular formation in the brain stem in higher vertebrates (Barreiro-Iglesias et al., 2008). In addition and common to all pretetrapod vertebrates a group of midline serotonergic neurons is present along the length of the spinal cord. These neurons project widely throughout the spinal cord cord, and strongly innervate both the spinal ventral horn and surround glutamatergic reticulospinal axons along the length of the spinal cord. Release from these neurons is paracrine in fashion and serotonin released in this way is believed to activate receptors on giant axons.

However, there is a lack of definitive studies directly showing such a relationship. This paracrine release of serotonin, as well as many of serotonin's functional roles, appears to be conserved. Serotonin's profound inhibitory effect on locomotor pattern generation has been documented in a large variety of vertebrates (Barbeau and Rossignol, 1990; Sillar et al., 1992; Sillar and Simmers, 1994). Additionally, owing to the unparalleled accessibility conferred by the lamprey giant reticulospinal axons and synapses, the lamprey is a superb model organism for studying the function of this neurotransmitter in a motor pathway.

Serotonin acts in a diffuse manner throughout the reticulospinal tract, a neuroanatomical pathway that emanates from the brainstem. Serotonin is a potent inhibitor of glutamate release in this system, but the details that have emerged suggest that the mechanism behind such inhibition affords the system a more nuanced level of regulation that allows neurons to modify glutamate output in response to changing levels of this neurotransmitter. There are 13 known 5-HT receptor subtypes, but only one of these has been shown to act at the presynaptic terminal, the 5-HT1b/1d receptor. A 5-HT1b/1d-like receptor is found in the giant reticulospinal axons of the lamprey (*P. marinus*), which is the model system under investigation in this dissertation. A downstream effector of all GPCRs is the heterodimer $G\beta\gamma$, which is released upon exchange of GDP for GTP by $G\alpha$. In the case of the 5-HT1b/1d receptor within the presynaptic terminal, $G\beta\gamma$ competes with synaptotagmin in a calcium-dependent manner, for access to target membrane SNAREs (t-SNAREs), the result of which is a modification in vesicle fusion with the presynaptic membrane and a subquantal

release of neurotransmitter (Blackmer et al., 2005; Gerachshenko et al., 2005; Schwartz et al., 2007; Yoon et al., 2007a).

Evidence for a shift from full fusion to kiss-and-run fusion following 5-HT1b/1d receptor activation has come from studies using paired recordings, as well as fluorescence microscopy studies utilizing styryl dyes, which provide a reliable index of vesicular turnover. 5-HT activates the 5-HT1b/1d receptor within minutes, which reduces glutamate release, and therefore the post-synaptic response. Specifically, AMPA and NMDA receptor components of the post-synaptic response are both dose-dependently reduced by 5-HT (Schwartz et al., 2007). Similarly, both uptake and release of styryl dyes such as FM1-43 through endocytosis and exocytosis, respectively, are affected by 5-HT's impact on vesicle fusion. Specifically, endocytosis as measured by loading of FM1-43 is diminished in 600nM 5-HT (Photowala et al., 2006), considered to be a half-maximal dose based on a dose response curve for 5-HT generated by the Alford lab (Schwartz et al., 2007); that is, at this dose, around 50% of the post-synaptic glutamatergic response remains. Thus, serotonin's inhibitory effects appear to be graded even at individual synapses; rather than causing a reduction in probability of release at individual synapses, serotonin reduces the amplitude of individual quantal events. In contrast, vesicle fusion during exocytosis as measured by FM1-43 fluorescence changes following 5-HT administration reveals a slightly different result. In this case, the FM1-43 dye is almost completely retained (Photowala et al., 2006). The marked difference between

dye loading which can be achieved in the presence of 5-HT and destaining which cannot, can be explained, in part, by the fact that FM1-43 is abundant in the bath during the loading protocol, so any dye that dissociates itself from the plasma membrane is readily replaced. In addition, because the dye is lipophilic, association with the membrane is thermodynamically favorable compared to aqueous solution. Finally, the duration of a transient/kiss-and-run fusion event, on the order of a few hundred milliseconds up to 2 seconds (He et al., 2006) is shorter than the off-rate for FM1-43 from lipid bilayers (Figure 1), which may explain why FM1-43 destaining is more substantially inhibited by a concentration of 5-HT that only partially blocks FM1-43 loading. Dye in the vesicle that is partially fused to the membrane, i.e., during transient/kiss-and-run fusion, cannot access the fusion pore, whereas dye in aqueous solution applied exogenously to the extracellular space does have this access.

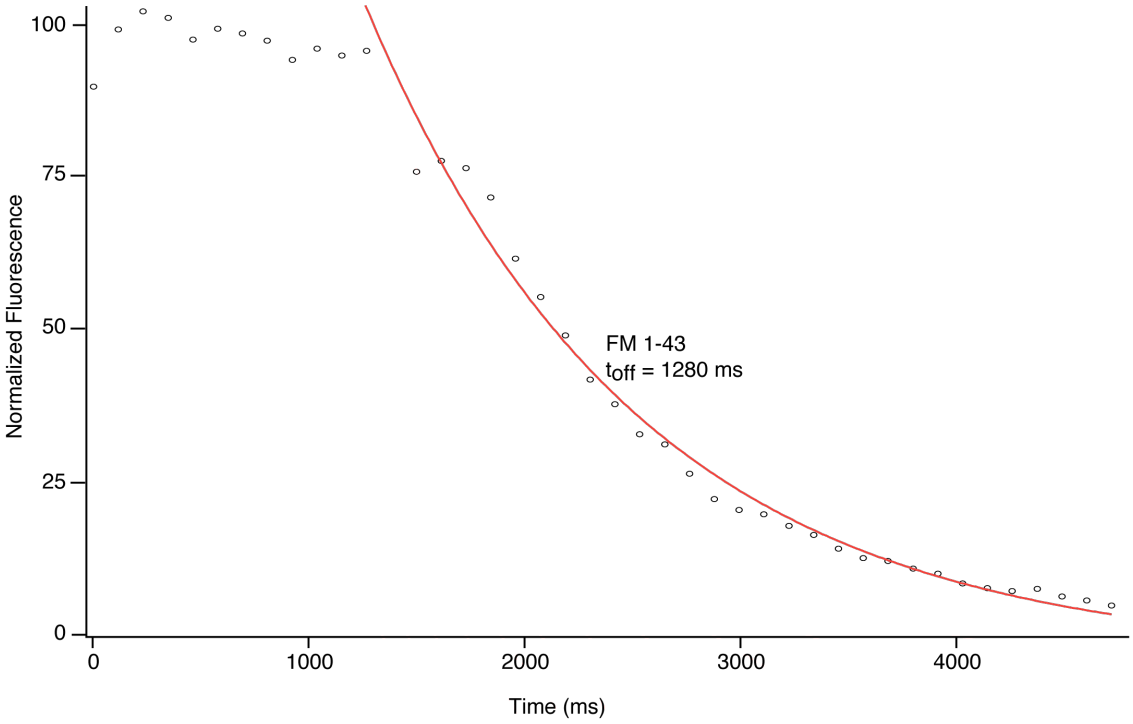

Borrowed from laboratory of Simon Alford, with permission

Figure 1. Decay of FM1-43 fluorescence from membrane partition. FM1-43 (4μM) dissolved in aqueous media was superfused onto tissue to allow association with the plasma membrane (1s), after which the dye flow was stopped. Fluorescence was measured throughout, showing that upon removal of the source of FM1-43, dye spontaneously dissociates from the membrane. (Unpublished data)

Activation of a 5-HT1b/1d-like receptor by 5-HT in the lamprey giant reticulospinal axon was been shown to occur by Gβγ binding to the C-terminal domain of SNAP-25 in the SNARE complex (Blackmer et al., 2001; 2005; Gerachshenko et al., 2005). This occurs at a site consistent with synaptotagmin binding the SNARE complex, and is further supported by the finding that 5-HT no longer inhibits neurotransmitter release after presynaptic injection of botulinum toxin A, which cleaves the nine most C-terminal residues of SNAP-25, nor after presynaptic injection of a peptide corresponding to the C-terminal 14 amino acids of SNAP-25 (Blackmer et al., 2005; Gerachshenko et al., 2005). Also, presynaptic injection of the C terminus of a G-protein receptor kinase-2, which acts as a scavenger of Gβγ, blocks 5-HT-mediated inhibition at the lamprey giant reticulospinal synapse (Blackmer et al., 2001). Finally, modification of interactions between synaptotagmin and SNARE complexes has been shown to cause incomplete fusion of dense core vesicles (Bai et al., 2004; Richards, 2005).

Clearly, activation of the 5-HT1b/1d-like receptor receptor in the lamprey giant reticulospinal axon prevents collapse of synaptic vesicles into the presynaptic membrane. This results in a reduction of quantal amplitude of excitatory postsynaptic currents (EPSCs) (Photowala et al., 2006; Schwartz et al., 2007). However, until recently, it was unclear whether this reduction was due to a change in the probability of release (Pr). Changes in synaptic cleft glutamate concentration were thought to occur after manipulations in Pr by multivesicular

release (Tong and Jahr, 1994) or spillover from other synapses (Asztely et al., 1997). However, such changes can also occur independently of vesicle fusion Pr after long-term potentiation (Choi et al., 2000). Incidentally, in cultured hippocampal neurons, the incidence of transient vesicle fusion events is reduced with increased stimulation frequency (Harata et al., 2006b). On the other hand, long-term depression has been shown to reduce the rate of FM1-43 dye destaining from fusing vesicles independently of Pr (Zakharenko et al., 2002). Recent studies, however, have shown that activation of the 5-HT1b/1d-like receptor in the lamprey giant reticulospinal axons lowers the peak synaptic cleft glutamate concentration independently of Pr, an effect which differentially inhibits synaptic NMDA- and AMPA-receptor-mediated currents (Schwartz et al., 2007).

1.3 Synaptic vesicle biogenesis

There are two major pathways that lead to the formation of *de novo* synaptic vesicles, both utilizing clathrin: 1) a plasma membrane budding pathway which utilizes a heterotetrameric clathrin adaptor complex AP2 and the large GTPase dynamin (Smillie and Cousin, 2005; Granseth et al., 2006; Jung and Haucke, 2007; Lu et al., 2009); and 2) "the endosomal pathway," which may include vesicle budding from both endosomes and the Golgi complex (Glyvuk et al., 2010; Körber et al., 2012), two types of membrane-bound organelles important in sorting contents and membrane composition of vesicles. Because the use of the two budding pathways in vesicle biogenesis is developmentally regulated with the latter being used primarily in immature neurons and following

bulk endocytosis, in which excess membrane is rapidly internalized from deep plasma membrane invaginations after a strong exocytic event (Takei et al., 2012), the focus of this introduction will be on the former.

1.3.1 Endocytosis

It is generally accepted that clathrin-mediated endocytosis (CME) is the major pathway for compensatory endocytosis and retrieval of synaptic vesicle membrane following full fusion with the presynaptic plasma membrane (Granseth et al., 2006; Harata et al., 2006a; Jung and Haucke, 2007; Rizzoli and Jahn, 2007; Dittman and Ryan, 2009; Mettlen et al., 2009; Takei et al., 2012). This process has been shown to occur in the "periactive zone," region named for its relation, and topographical relationship, to sites of release (the synaptic active zones) (Verstreken et al., 2002; Shupliakov and Brodin, 2010; Sundborger et al., 2010). The key components of this molecular mechanism, clathrin, AP2, and dynamin, are part of a coat complex in the very early stages of clathrin vesicle assembly, the recruitment of which involves interactions with cell membrane constituents such as phosphoinositides, as well as synaptotagmin and other accessory proteins (Takei et al., 2012). Induction of membrane curvature, resulting clathrin-adaptor-lipid interactions is crucial to budding vesicle formation (Takei et al., 1998; Ford et al., 2002). During formation of the clathrin lattice, other binding partners involved in vesicle formation are recruited, including epsin (Ford et al., 2002), endophilin (Verstreken et al., 2002; 2003; Sundborger et al., 2010), and amphiphysin (Wigge and McMahon, 1998; Hartig et al., 2009; Wu et

al., 2009; Yamada et al., 2009), which are involved in membrane sculpting and clathrin rearrangements.

Formation of vesicles also involves scission of any remaining membranous attachment to the plasma membrane. The core of this scission complex is dynamin (Pucadyil and Schmid, 2009). In addition, it has been shown with total internal reflection microscopy that during fission, dynamin recruitment to clathrin-coated pits (CCPs) is rapidly followed by the recruitment of actin and dynamin-interacting accessory proteins important in promoting constriction of the vesicle neck (Merrifield et al., 2005; Ferguson et al., 2009). As its name suggests, CME is defined, in part by the role clathrin plays in the process of invaginating cellular membrane leading to omega formations (so named for the resemblance of these ultrastructural morphologies to the Greek letter "Ω"), membrane tubulation, and finally vesicle scission culminating in a "free" vesicle. Clathrin polymerizes in a cage-like structure around budding vesicles (Doxsey et al., 1987; Granseth et al., 2006), but a fully formed vesicle requires clathrin's tightly regulated interactions with adapter proteins, such as endophilin (Ringstad et al., 2001; Verstreken et al., 2002; Granseth et al., 2006; Anggono and Robinson, 2007; Sundborger et al., 2010), amphiphysin (Shupliakov et al., 1997; Wigge and McMahon, 1998; Yoshida and Takei, 2005; Lu et al., 2009; Wu et al., 2009), and dynamin (Hinshaw and Schmid, 1995; Praefcke and McMahon, 2004; Smillie and Cousin, 2005; Macia et al., 2006; Nankoe and Sever, 2006; Newton et al., 2006; Thompson and McNiven, 2006; Kirchhausen et al., 2008; Lu et al.,

2009; Mettlen et al., 2009; Sundborger et al., 2010; Douthitt et al., 2011; Schmid and Frolov, 2011). Specifically, individual triskelions composed of three heavy chains radiating outward from a c-terminal trimerization domain, with a clathrin light chain attached to each of the three radiating branches, form the basic building block of the clathrin coat (Doxsey et al., 1987). These structural building motifs assemble around the semi-spherical vesicle that buds from the presynaptic membrane.

Finally, following vesicle budding, the clathrin coat is rapidly removed, a reaction that is dependent on adenosine triphosphate (ATP), a common cellular source of energy, and requires binding partners such as synaptojanin-1 and auxilin (Wenk and Pietro P De Camilli, 2004; Dittman and Ryan, 2009). While many players in the vesicle cycle are known—e.g., dynamin, clathrin, clathrin adaptor proteins, synaptojanin, synapsin, and syndapin, to name a few—the functional relationships amongst them vary slightly depending on the system one analyzes. Not only do consideration of isoform variants in different species play a role, but also availability of membrane varies in different synapses. Thus, interpretations of data derived from any one system must be cast with a degree of circumspection.

The study of endocytosis has been advanced by a vast array of peptides and pharmacological agents targeting specific proteins in this cascade. For example, antibodies against certain regions of clathrin can be applied to cells under stimulation to arrest endocytosis (Doxsey et al., 1987). Likewise, many of

the binding partners, e.g., amphiphysin and endophilin, have also been targeted as a means of disrupting endocytosis (Wigge and McMahon, 1998; Ringstad et al., 2001; Verstreken et al., 2002; Yoshida and Takei, 2005; Wu et al., 2009; Sundborger et al., 2010). In addition, electrophysiology provides a functional readout for studies of endocytosis, given that neurotransmitter release in paired cells is tightly coupled to vesicle activity. Furthermore, with current fluorescence microscopy techniques, e.g., styryl dies, evidence of vesicle turnover can be studied as a function of fluorescence change in response to various challenges to endocytosis (Cochilla et al., 1999).

Regulation of cellular traffic across the cell membrane and maintenance of both cellular membrane area and vesicle pools is dependent on a balance between endocytosis and exocytosis. Release of neurotransmitter from small clear vesicles in cellular domains such as presynaptic terminals necessitates membrane turnover. In presynaptic terminals, this turnover has been shown as fluctuations in fluorescence with the use of fluorescent dyes taking advantage of pH changes in vesicle lumen at various stages of vesicle fusion or formation under stimulation (Zhu et al., 2009); styryl dyes, such as FM1-43, which can also be used as indices of endocytosis and exocytosis (Betz et al., 1992b; 1993; Pieribone et al., 1995; Henkel et al., 1996; Wang and Zucker, 1998; Cochilla et al., 1999; Cousin and Robinson, 1999; Liao et al., 2002; Aravanis et al., 2003a; Stanton et al., 2005; Anggono et al., 2006; Groemer and Klingauf, 2007; Gitler et al., 2008; Chung and Kavalali, 2009; Zhu et al., 2009); and capacitance changes

during and after vesicle fusion and formation (He and Wu, 2007). In some simplified systems, e.g., semi-intact preparations, and cultured cells making synaptic contact, disruption of the vesicle cycle through pharmacological blockade of endocytosis or exocytosis leads to abolishment of neurotransmitter release. This is a reflection of the tight coupling between endocytosis and exocytosis that impacts the availability of vesicles and plasma membrane.

1.3.2 Dynamins

Dynamin belongs to a group of guanosine triphosphatases (GTPases) known as the dynamin superfamily, which includes classical dynamins, dynamin-like proteins, Mx proteins, OPA, mitofusins, and GBPs. These proteins have functions ranging from vesicle scission (classical dynamins, ADL6 in plants) to organelle division (dynamin-like proteins (Dlp's)/Dnm1) to cytokinesis and mitochondrial division (ADL1A, ADL2B in plants) (Praefcke and McMahon, 2004). All of these functions involve formation from, or dissolution of, membrane bound compartments, including membrane tubulation and/or scission.

Dynamins have been classified as large GTPases to distinguish them form the small Ras-like GTPases, as well as other regulatory GTPases, including the α-subunits of heterotrimeric G-proteins and the translation factors of protein biosynthesis (Praefcke and McMahon, 2004). These GTPases share the common functional stipulation that their GTPase domains become active upon oligomerization. In the case of classical dynamins, activation of the GTPase domain results in GTP hydrolysis, as well as dissociation of dynamin monomers

from the oligomerized ring-like structure. It is unclear as to how precisely classical dynamins regulate vesicle scission, but this function appears to depend on interactions with binding partners such as endophilin (Mettlen et al., 2009; Wu et al., 2009; Sundborger et al., 2010; Faelber et al., 2012) and amphiphysin (Lu et al., 2009; Yamada et al., 2009). Thus, dynamin's depolymerization and its membrane and protein interactions conducive to vesicle scission are competing processes, both of which are driven by GTP hydrolysis. Thus, details of vesicle scission and its dependence on GTP hydrolysis remain to be elucidated.

Dynamin family proteins also all appear to interact with lipid membranes. Elucidating these roles has been possible with the use of non-hydrolysable analogues of GTP, such as GTP*γ*S; constitutively active analogues of GDP, such as GDPβS; pharmacological agents targeting the GTPase domains, preventing or slowing GTP hydrolysis; peptides based on the proline-rich domains (PRDs) of dynamins to which proteins expressing a particular tyrosine-protein kinase gene found in sarcoma cell lines, i.e., a SRC homology 3 (SH3), domain; and genetic mutations to the genes encoding dynamin isoforms, e.g., *shibire* mutants (Kuromi and Kidokoro, 1998; Delgado et al., 2000; Praefcke and McMahon, 2004; Büschges et al., 2011).

Dynamin-2, one of the classical dynamin isoforms, has been shown to have a regulatory effect on membrane remodeling and cytoskeletal remodeling (Praefcke and McMahon, 2004; Roux et al., 2006; Schmid and Frolov, 2011; Faelber et al., 2012). The PRD of dynamin's C-terminal domain has been shown

to interact with SH3 domains of actin, neural–Wiskott–Aldrich syndrome protein (N-WASP) (Hartig et al., 2009; Yamada et al., 2009; Galletta et al., 2010), and Arp2/3 complex (Ferguson et al., 2009; Galletta et al., 2010), and many of these interactions have been shown to be important in membrane remodeling. Membrane remodeling underlies cell migration, cell division, and neurite growth and collapse during development, all of which are processes that occur over time scales that dwarf what occurs during synaptic transmission (Wagh et al., 2006; Ferguson et al., 2009; Sundborger et al., 2010). Stabilization of filamentous actin (F-actin) via the toxin phalloidin prevents turnover of actin and has a subsequent effect of abolishing neurotransmission, while disruption of polymerization of actin via latrunculin does not disrupt neurotransmission (Bleckert et al., 2012). Thus, it is speculated that two structurally and functionally distinct pools of actin exist at presynaptic sites.

However, it remains unknown what relationship exists between vesicle cluster stability and endocytic proteins such as dynamin, amphiphysin, endophilin, synaptojanin, clathrin, and/or AP-2. Dynamin-2 has been shown to regulate actin comet formation in HeLa cells, but this interaction appears to be intimately linked to endocytic function (Henmi et al., 2011). Cytoskeletal regulation, to be sure, is known to have an impact on vesicle activity. Cortical actin, that is, actin filaments that have organized just beneath the plasma membrane, has been shown to present a barrier to vesicle association with the membrane (Bleckert et al., 2012; Gutierrez, 2012).

Dynamin-1, -2, and -3 represent some of the classical dynamins within the dynamin superfamily of GTPases (Praefcke and McMahon, 2004). Others include shibire/dynamin-like protein 1 (Dlp1) in the fruit fly, *D. melanogaster* (Kuromi and Kidokoro, 1998; Delgado et al., 2000; Wu et al., 2009; Takei et al., 2012), and ADL6 in plants, e.g., *A. thaliana* (Lam et al., 2002). The classical dynamins mediate vesicle scission, and are localized to the plasma membrane, trans-Golgi network, and endosomes. Dynamin-1 and -2 are the known isoforms mediating a critical role in CME in neurons, while dynamin-3 is present in testes, heart, brain, and lung tissues. Dynamin-1 and -2, considered the main neuronal isoforms of dynamin.

Dynamin monomers oligomerize when they are bound to guanosine triphosphate (GTP) (Pieribone et al., 1995; Sundborger et al., 2010). Oligomerization results in ring-like structures that lead to tubulation of membranes (Praefcke and McMahon, 2004; Anggono et al., 2006; Kessels, 2006; Sundborger et al., 2010). The precise mechanism is still unknown, and there are several binding partners to these neuronally dominant isoforms. Endophilin, synaptojanin, and amphiphysin all appear to play a critical role in recruiting dynamin to sites of endocytic activity, but also may regulate the GTPase activity of dynamin (Pieribone et al., 1995; Shupliakov et al., 1997; Wigge and McMahon, 1998; Ringstad et al., 2001; Bloom, 2003; Kessels, 2004; Smillie and Cousin, 2005; Yoshida and Takei, 2005; Sundborger et al., 2010; Taylor et al., 2012).

Upon activation of the GTPase domain in dynamin, GTP is hydrolyzed and loses a phosphate to become guanosine diphosphate (GDP). GDP-bound dynamin monomers have a lowered affinity for each other, and thus the ring-like oligomers depolymerize, leaving free GDP-bound dynamin monomers. GTP is has been shown to be constitutively loaded onto dynamin monomers, but the protein is sensitive to the energy status of the cell. This is in contrast to Ras-like GTPases, which utilize guanine nucleotide exchange factors (GEFs) to replace GDP with GTP. Furthermore, GTPase activation is dependent on oligomerization of dynamin dimers and tetramers, the basic dynamin building blocks. In contrast, Ras-like GTPases require GTPase activating protein (GAPs). Dynamin, thus, is essentially its own GAP. However, GTPase activation also has been shown to lead to constriction of the ring-like structures discussed above, which is thought to be crucial to the severing of the remaining tubulated membrane during CME. One model of vesicle scission is based on findings that suggest that in the absence of nucleotide, dynamin assembles in a relaxed conformation around tubular membrane templates. Upon binding of GTP, conformational changes then induce constriction of the oligomer followed by membrane scission (Hinshaw and Schmid, 1995; Chen et al., 2004b; Mears et al., 2007) (the “constrictase” model). However, it was discovered that the dynamin helix is more closely packed in the GTP-bound form and opens upon hydrolysis of GTP to GDP (Stowell et al., 1999) This led to a model in which the dynamin helix opens like a spring upon nucleotide hydrolysis (the “poppase” model). Roux et al (2006)

showed further that GTP hydrolysis results in twisting of dynamin-coated membrane tubules during vesicle scission (the “twistase” model). Thus, it is unclear based on the variety of systems assayed which model best explains dynamin’s mechanism of action. Additionally, recent evidence suggests another binding partner in the CME pathway could play a decisive role in vesicle scission adding another level of regulation of vesicle scission to what is currently known.

Recent evidence also suggests epsins may play a more crucial role in vesicle scission than dynamin alone (Boucrot et al., 2012). For example, in cells depleted of dynamin, Boucrot et al (2012) used epsin to rescue vesicle scission. Thus, while vesicle scission in higher eukaryotes has been shown to be primarily carried out by dynamin, there is evidence that epsin also plays a crucial role. However, membrane budding in the early phases of endocytosis is not supported by epsin when dynamin activity is blocked by drugs such as dynasore, a GTPase inhibitor or dynamin-1 and -2; in cells treated with dynasore, dynamin accumulates in the neck of clathrin-coated structures (CCSs). It has been proposed that epsin may provide the required force to destabilize necks of recently formed vesicles. Meanwhile, the scaffolding generated by dynamin oligomerization could provide a time-sensitivity to membrane scission mediated by cooperative GTP-hydrolysis mediated depolymerization. Interpretations of the findings of this thesis, with respect to dynamin, will be cast in light of these findings. This will lead to potential new targets of study of endocytosis and

vesicle cycle regulation at the presynaptic terminal and elsewhere, as well as, studies that can further elucidate or clarify the results herein.

Turnover of synaptic vesicles has been studied at several points of synaptic contact, including frog neuromuscular junction (Betz et al., 1992a; 1992b; 1993; Betz and Bewick, 1993), *en passant* synapses on reticulospinal neurons (Rossi et al., 1995; Blackmer et al., 2005; Gerachshenko et al., 2005; Photowala et al., 2005; 2006; Schwartz et al., 2007; Yoon et al., 2007a; Gerachshenko et al., 2009b), synapses at the Calyx of Held (Wu and Wu, 2009; Körber et al., 2012; Yao and Sakaba, 2012), and many more. While endocytosis and exocytosis are inextricably linked, there is a spectrum of findings that reveal nuances of these cellular functions. For instance, bulk endocytosis has been shown to be proportional to firing rate of a given neuron, with higher firing rates leading to greater neurotransmitter release via exocytosis, and subsequent bulk endocytosis.

Understanding the mechanism of vesicle retrieval following a kiss-and-run fusion event was the impetus behind a portion of this thesis. As discussed, clathrin-mediated endocytosis employs a complex protein cascade involving several binding partners, which served as a starting point for our investigation. An attractive protein target is dynamin. I began my work in the laboratory of Simon Alford, focusing on whether a dynamin-1/2-like protein in the lamprey was responsible for vesicle scission following a transient/kiss-and-run vesicle fusion event.

To release their contents into the synaptic cleft, in the case of presynaptic terminals, vesicles must fuse with the plasma membrane. The quantal theory of neurotransmission (Fatt and Katz, 1952; del Castillo and Katz, 1954) states that neurotransmitter molecules are released in discrete packets. Furthermore, the vesicle theory states that vesicles gauge the amount of transmitter that generates a miniature signal (quantum) and that vesicular exocytosis is the mechanism by which this quantum is entirely discharged in the synaptic cleft following Ca^{2+} entry (Vautrin and Barker, 2002). During kiss-and-run fusion, a fully formed vesicle only briefly fuses with the target membrane, without fully collapsing into the membrane as it would during a full fusion event. Kiss-and-run events have been shown to occur in milliseconds, whereas vesicle formation from clathrin-mediated endocytosis occurs over a much longer time scale. Thus, it is more likely that the mechanism to allow retrieval of a vesicle following kiss-and-run would incorporate some, but not all, of the same machinery as CME, a process that begins with a signal that leads to invagination of membrane, incorporating structural changes in cytoskeletal proteins, e.g., actin, not to mention the array of proteins involved downstream in later CME processes, e.g., clathrin, dynamin, synaptojanin, endophilin, AP-2. Thus, plasticity is conferred to synapses by a variety of distinct mechanisms.

Changing quantal output from individual vesicles presynaptically, modulating neurotransmitter availability in the synaptic cleft, and/or regulation of receptor sensitivity or availability post-synaptically, are just some of the ways in which adaptive responsiveness is conferred on the synapse, generating a

sophisticated, nuanced level of regulation that begins to elucidate the mechanisms involved in the relationship between the central nervous system and a continuously changing environment. The CNS has a large repertoire of regulatory mechanisms that are beginning to be understood. Studies in the field of neuroplasticity have illuminated distinct mechanisms of adaptation, but the data are far from clear.

It is still unclear as to what components of endocytosis are shared between CME and kiss-and-run fusion events (Figure 2). It has been suggested that the persistence of neurotransmission at the neuromuscular junction in *D. melanogaster* mutants in which CME is abolished via mutations in the genes for endophilin and synaptojanin, is due to kiss-and-run fusion (Verstreken et al., 2002; 2003). Endophilin and synaptojanin are two proteins thought to regulate uncoating of clathrin-coated vesicles (CCVs). However, subsequent studies suggest that a slowed classical endocytic pathway explains this persistence (Dickman et al., 2005). Not surprisingly, kiss-and-run fusion has remained a point of contention in the neuroscience community. Currently, details continue to emerge to elucidate to what extent this explains synaptic plasticity.

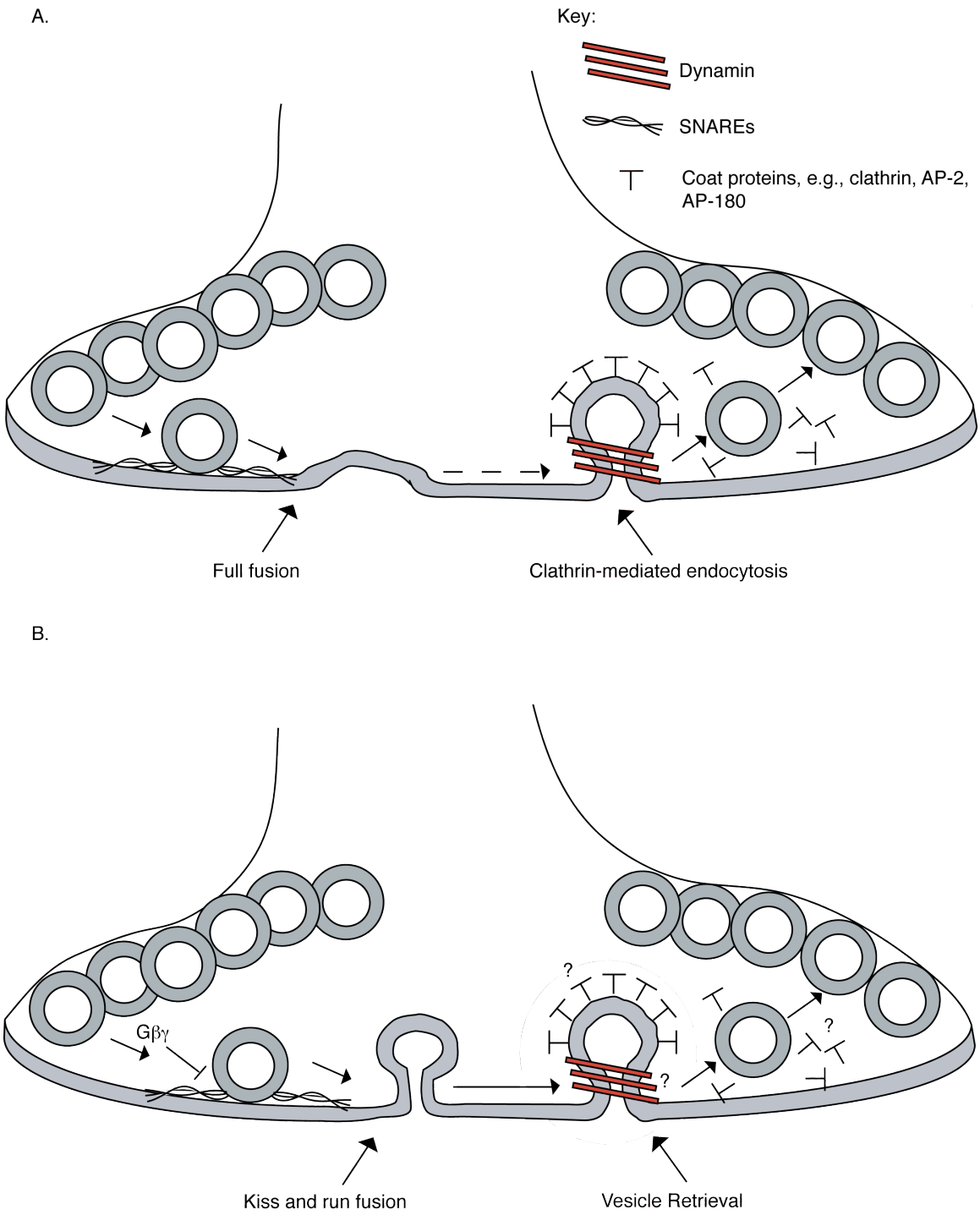
A.
Key:
Dynamin
SNAREs
Coat proteins, e.g., clathrin, AP-2, AP-180
Full fusion
Clathrin-mediated endocytosis
B.
Gβγ
?
?
?
Kiss and run fusion
Vesicle Retrieval

Figure 2. Schematic of vesicle cycle at presynaptic terminals. A. Full vesicle fusion implicating vesicular and target-membrane SNAREs (left side of terminal). Classical CME implicating coat proteins during budding and dynamin during vesicle scission (right side of terminal). B. Kiss-and-run vesicle in 5-HT-mediated presynaptic inhibition; $G\beta\gamma$ targeting synaptotagmin's binding site on the SNARE complex is indicated. Unclear involvement of components of CME, e.g., dynamin, clathrin, and other coat proteins, is indicated by question marks.

While some hold to the notion of the controversial status of this putative contributor to the CNS's repertoire of adaptive responses, due to an abundance of data from carefully controlled studies in a variety of settings, this is a measureable, reliable, and physiologically valid component of plasticity in the field of neuroscience. As such, it was considered a worthy task to determine if a particular CME-related protein, dynamin, is involved in kiss-and-run fusion

Because the focus of this thesis is on dynamin's role in resting and active presynaptic terminals, factors implicated in CME will be discussed as they relate to dynamin. As the following chapters will illustrate, the pursuit to answer the question of whether dynamin, a protein with a strongly supported role in CME, might also play a role in kiss-and-run fusion as presented in Chapter 3, revealed a conundrum that has led to a host of other findings that may further our understanding of dynamin's function(s) outside of classical endocytosis (presented in Chapter 4).

Vesicle pools are maintained by a variety of mechanisms, the details of which are still unclear. Vesicle formation is essential to replenish vesicle pools, while vesicle fusion is essential for the contents--either membrane-bound or the soluble cargo of a secretory vesicle—to reach their subsequent destination. Tight regulation of protein-protein interactions with target membrane—Golgi, lysosomes, plasma membrane—is orchestrated by SNARE proteins (Schiavo et al., 1997; Sudhof, 2000; Deak et al., 2004; Rickman et al., 2004; Verderio et al., 2004; Blackmer et al., 2005; Chen et al., 2005a; Schwartz et al., 2007; Yoon et

al., 2007a), whereas regulation of vesicles ready for release is dependent on interactions with filamentous cytoskeletal proteins, such as actin (Bloom, 2003; Gaffield et al., 2006; Galletta and Cooper, 2009; Galletta et al., 2010; Bleckert et al., 2012; Mooren et al., 2012; Taylor et al., 2012). The fourth chapter presents results addressing the question of whether dynamin is important in maintaining a pool of vesicles in a resting presynaptic terminal.

2. MATERIALS & METHODS

2.1 Animal Model

Experiments were performed on spinal cords dissected from larval lampreys (*Petromyzon marinus*) that were anesthetized with ethyl 3-aminobenzoate methanesulphonate salt added to aquarium water (MS-222; 100 mg/liter; Sigma-Aldrich) and sacrificed by decapitation. Dissections were performed in cold standard lamprey Ringer (approximately 10°C; 100 mM NaCl/2.1 mM KCl/2.6 mM CaCl2/1.8 mM MgCl2/4 mM glucose/5 mM Hepes), adjusted to pH 7.6 with 1 M NaOH. Decapitation was followed by further dissection of the remaining muscular tissue of the body, as well as the integument of the spinal cord, the mininx primtiva, which leaves an intact spinal cord isolated in in vitro conditions. The tissue was then pinned ventral surface up to expose the ventrally coursing giant reticulospinal axons for both electrophysiological recording and imaging in a temperature-controlled (10°C) chamber in which cold saline is superfused over the tissue. This arrangement allows the maintenance of the intact spinal cord section's viability for over 24 hours (Kay et al., 1999). The advantage of using larval lamprey spinal cords, and in particular the giant reticulospinal axons therein, is that it offers unparalleled access to presynaptic structures within the axons (Kay et al., 1999). In particular, the spinal cord is only 150µm thick, with unmyelinated axons, making it ideal for imaging studies. Furthermore, much of the length of the structure is traversed by giant axons with diameters of up to 50µm, which are unique in that they have few, if any, morphological features of the presynaptic

elements found in other tissue—e.g., brain slice cultures—but rather clusters of synaptic vesicles immediately adjacent to contiguous, undeviated axonal membrane (Wickelgren et al., 1985).

2.2 Electrophysiology & Imaging

Sharp electrodes were used to stimulate and record the membrane potential of reticulospinal axons in standard lamprey Ringer. Axons were recorded with microelectrodes containing 1-3M KCl (20-30 MΩ) or 1M KMeSO4 (30-60MΩ). Cell bodies of neurons were recorded with patch electrodes containing 102.5 Cs methane sulfonate, 1mM NaCl, 1mM MgCl2, 5mM EGTA, and 5mM Hepes, pH adjusted to 7.2 with CsOH. For loading of FM1-43 (Figure 1A), axons were stimulated (0.5 - 5Hz, 2000 stimuli) in the presence of FM1-43 (4μM), and cleared with Advasep-7 (1mM, 10min) followed by washing out with lamprey Ringer (10 min). Advasep is a modified cyclodextran that has been shown to act as a carrier molecule (Szejtli, 1998) that has a higher affinity for FM1-43 than membranes and efficiently removes FM1-43 from the extracellular space, allowing it to be washed away, greatly reducing background staining. Without this clearing agent, it would not be possible to image synapses in tissue because nonspecific binding of FM1-43 would obscure the visualization of synaptic terminals. It has previously been shown that this protocol loads clusters of vesicles (represented by puncta in fluorescence micrographs) and that the resulting fluorescence of puncta is significantly higher than background fluorescence (Kay et al., 1999; Photowala et al., 2006). Post-synaptic uptake of

FM1-43 through activation of NMDA and AMPA receptors during loading was blocked by bath application of DL-AP5 (100μM) and CNQX (10μM), respectively (Alford and Grillner, 1990). Without such pharmacological blockade, postsynaptic neurons are also loaded with FM1-43 upon stimulation of presynaptic axons onto which they synapse, greatly increasing fluorescence not specific to the original reticulospinal axon being stimulated.

Dye-stained axons were imaged confocally (modified Bio-Rad MRC 600) or conventionally (Hamamatsu charge-coupled device). Staining is synapse-specific, with clusters of vesicles appearing as punctate structures along the axon (Photowala et al., 2005). Using ImageJ (National Institute of Mental Health, Bethesda, MD), a *z*-stack of 3 images, 2μm apart in the *z*-plane was collected at select time points and averaged. This allows for corrections in any deviation of the focal plane due to unavoidable microscope thermal instability during the extended course of these experiments. Drug-dependent changes in fluorescence values over time were evaluated in tissue at rest and/or under stimulus-dependent destaining conditions. Stimulus-dependent FM1-43 destaining was achieved using the same respective stimulation frequency as that for FM1-43 loading.

2.3 Pharmacological Reagents

6-cyano-7-nitroquinoxaline-2,3-dione (CNQX) is a potent and selective antagonist of non-N-methyl-D-aspartate (NMDA) receptors in the mammalian nervous system. In the lamprey, CNQX has been shown to block fast excitatory

synaptic potentials elicited in neurons of the spinal ventral horn (Alford and Grillner, 1990), particularly post-synaptic neurons which would be otherwise loaded with FM1-43 (see above). CNQX sodium salt (Tocris) was prepared by dissolving the salt in deionized water (final resistance of ≤ 16.7MΩ), yielding aqueous aliquots (10mM, 100µL) and maintained at -20°C. These aliquots were then dissolved in fresh lamprey Ringer to a final concentration of 10µM.

DL-2-amino-5-phosphonopentanoic acid (DL-AP5) is a selective NMDA receptor antagonist that completely inhibits the binding site of NMDA receptors (Davies and Watkins, 1982). This is important in blocking activity of post-synaptic neurons that would otherwise be loaded with FM1-43. DL-AP5 sodium salt (Tocris) was prepared by dissolving the salt in deionized water (final resistance ≤ 16.7MΩ), yielding aqueous aliquots (100mM, 100µL) and maintained at -20°C. These aliquots were then dissolved in fresh lamprey Ringer to a final concentration of 100µM.

Strychnine is a convulsant and glycine receptor antagonist not associated with the NMDA receptor. Without this agent, glycinergic inhibitory events would occur, thus contaminating recordings of pure glutamatergic EPSCs. Strychine (Sigma-Aldrich) was prepared by dissolving the salt in deionized water (final resistance ≤ 16.7MΩ), yielding aliquots (5mM, 1mL) and maintained at -20°C. These aliquots were then dissolved in fresh lamprey Ringer to a final concentration of 5µM.

Tetrodotoxin (TTX) is a potent neurotoxin that blocks action potentials by

binding to voltage-gated sodium channels in nerve cell membranes (Kao, 1972). TTX citrate salts were dissolved in deionized water (final resistance of ≤ 16.7MΩ), yielding aliquots (1mM, 100µL) and maintained at -20°C. These aliquots were dissolved into fresh lamprey Ringer to a final concentration of 1µM. This drug prevents evoked neurotransmitter release, which is an important set of controls to maintain during studies of spontaneous mini-excitatory post-synaptic responses.

5-hydroxytryptamine (Sigma-Aldrich) was prepared by dissolving serotonin/5-HT HCl salts into deionized water (final resistance of ≤ 16.7MΩ), yielding aqueous aliquots (1mM, 100µL) and maintained at -20°C. These aliquots were then dissolved into fresh lamprey Ringer to a final concentration of 600nM in deionized water. This is a half-maximal dose based on dose-response curves generated from paired recordings in the Alford laboratory (Schwartz et al., 2004); that is, this is the dose at which 48.65 ± 8.05% of synaptic transmission was blocked. 5-HT was bath applied to the semi-intact spinal cord preparations prior to, and during, stimulation, and/or in resting conditions, depending on the experiment.

Dynasore is an inhibitor of the GTPase domain of dynamin-1 and -2, as well as dynein-1 and -2 (Macia et al., 2006). Dynasore monohydrate salt (Sigma-Aldrich) was prepared by dissolving the salt in 75% dimethyl sulfoxide (Sigma-Aldrich) into 40µL aliquots, which were then dissolved in lamprey Ringer to a final concentration of 20µM. This is the minimum concentration at which dynamin

inhibition has been recorded in previous studies (Macia et al., 2006; Nankoe and Sever, 2006; Newton et al., 2006; Thompson and McNiven, 2006; Kirchhausen et al., 2008; Lu et al., 2009; Wu et al., 2009; Lee et al., 2010; Douthitt et al., 2011).

Dynamin inhibitory peptide (Tocris) was prepared by dissolving the peptide to a final concentration of 1mM in deionized water purified to a final resistance of ≤ 16.7MΩ, and 20µL aliquots were maintained at -20°C. Aliquots were dissolved in 3M KCl to a final concentration of 500µM and pressure-injected (one 300ms pulse/minute for 10 minutes) into axons when appropriate, and allowed to rest for ≥ 10 minutes prior to any further manipulation. Due to the unparalleled access of the lamprey giant reticulospinal axon, pressure injection of this peptide was regarded as an advantage over the much costlier and nonspecific administration of a myristoylated version of the same peptide.

Botulinum neurotoxin B light chain (List Biological Laboratories) was dissolved to a final concentration of 200µM in deionized water purified to a final resistance of ≤ 16.7MΩ. Aliquots were further dissolved in 2M potassium methanesulfonate ($KMeSO_4$) to a final concentration of 100µM and pressure-injected (one 300ms pulse/minute for 10 minutes) into axons when appropriate, and allowed to rest for ≥ 10 minutes prior to any further manipulation. Using the light chain of this clostridial toxin is remarkably safer than using the complete toxin consisting of both heavy and light chains, and again, because of the unparalleled access of the lamprey giant reticulospinal axons, it is possible to directly inject the light chain of this toxin into these axons.

2.4 Fluorescence Analysis

Following averaging of a z-stack of confocal images (described in 2.1.1), FM1-43 fluorescence was measured at select time points in Image J (NIH, described in 2.1.1) by selecting a region of interest containing 5-10 puncta. Fluorescence intensity values at each time point were determined for selected puncta in the ROI, followed by subtracting representative background areas nearest to the puncta, respectively. These adjusted values are then expressed as percentage of the initial baseline fluorescence values. Between-group and within-group comparisons were made using Student's t-test, with $p < 0.05$ being the minimum standard for significance.

2.5 Quantal Analysis

Mini-EPSCs (inward current) above a minimum threshold were detected using an algorithm (Igor Pro), before and after drug application. Reticulospinal axons and ventral horn neurones (motoneurones or interneurones), identified by their location in the tissue and by capacity transients given by 10 mV voltage steps, were whole-cell clamped (with an Axopatch 200A amplifier, Axon Instruments) using a modified blind technique (Blanton et al., 1989; Cochilla and Alford, 1997). Patch pipettes had resistances around 5-10MOhm. Series resistance was continuously monitored by giving a 10 mV voltage step before each episode, and if the change exceeded 15%, the cell was discarded. Mini EPSCs were recorded in whole cell voltage clamp mode. For each time domain a total of 15s of data was obtained sampling at 5KHz.

To isolate only glutamatergic EPSCs during the recording glycinergic

inhibitory events were blocked with saturating dose of strychnine (5μM). The neurons were recorded at a holding potential of -70mV.

For analysis a sample of the control data prior to test peptide application were loaded into IGOR pro and analysis procedure used to detect events. Briefly in this procedure, sampled data was first filtered with a 9-point low-pass box filter, and the resultant data wave differentiated. A threshold detector was applied to the differentiated data set and all events exceeding this threshold were detected. The detected amplitude and time points were then overlaid over the original data set to confirm the adequacy of detection criteria. If acceptable, these threshold values were applied to all subsequent data and the detected events then used for comparison. Detected events were then displayed as binned frequency or event amplitude histograms (cumulative and standard) and significance of any changes determined by application of a Kolmogoroff-Smirnoff test applied as the maximum difference between drug and control data expressed as cumulative histograms. These tests were applied both to control and drug test data in individual cells and to data normalized to control response frequencies and amplitudes and combined across all sampled neurons.

Significance was determined using Student's paired *t* test. *P* values above 0.05 were determined not to be significant.

3. DYNAMIN IS NOT REQUIRED DURING EVOKED COMPENSATORY ENDOCYTOSIS IN THE PRESENCE OF 5-HT

3.1 Introduction

At lamprey reticulospinal axons, 5-HT does not modify release Pr, but instead liberates presynaptic Gβγ, to compete with Ca^{2+}-dependent synaptotagmin binding to soluble N-ethylmaleimide-sensitive factor attachment protein receptor (SNARE) complexes (Blackmer et al., 2001; 2005; Gerachshenko et al., 2005). This is known to cause kiss-and-run fusion (Photowala et al., 2006), and reduce cleft glutamate concentration (Schwartz et al., 2007). It remains unclear whether synaptic vesicle recycling during kiss-and-run fusion utilizes the same protein-protein interactions and lipid recycling pathways as has been defined for clathrin-mediated recycling that clearly occurs in lamprey giant synapses following extended periods of stimulated exocytosis (Brodin et al., 1994; Pieribone et al., 1995; Shupliakov et al., 1997; Jarousse and Kelly, 2001; Gustafsson et al., 2002; Verstreken et al., 2002; Evergren et al., 2006; Shupliakov and Brodin, 2010). Indeed, it is not at all clear what requirements exist for reconstitution of synaptic vesicle proteins or whether the vesicle loses identity during exocytosis.

Dynamin is believed to act as a 'pinchase' during CME (Morgan et al., 2002). Therefore, it represents a target to determine whether the endocytosis of vesicles undergoing recycling during kiss and run fusion follows the same pathway as during CME. Utilizing the pharmacological activation of kiss-and-run fusion in bath-applied 5-HT, I have used compensatory exocytosis in the

presence of 5-HT to probe the role of dynamin during kiss-and-run associated endocytosis.

3.2 Results

3.2.1 5-HT-mediated inhibition of AMPA-receptor mediated EPSCs is lost during train stimulation of the presynaptic axon

Because $G\beta\gamma$ released by presynaptic 5-HT1b receptor activation competes with Ca^{2+}- dependent synaptotagmin binding, at high [Ca^{2+}], there is preferential synaptotagmin binding to SNARE complexes, which occludes 5-HT-mediated inhibition (Yoon et al., 2007a). It has been proposed that kiss-and-run fusion is Ca^{2+}-dependent and is modified by high-frequency stimulation (Artalejo et al., 1998a; Harata et al., 2006b; Zhang et al., 2009). Thus, it was first necessary to determine whether repetitive stimulation can modify the mode of vesicle fusion to outline criteria for stimulation used to evoke synaptic transmission and kiss and run fusion in the presence of 5-HT. In line with this proposal, using paired recordings between reticulospinal axons and their ventral horn neuron targets, I determined the effect of 5-HT on synaptic AMPA receptor responses (EPSCs). Presynaptic and postsynaptic axons and cells were recorded in voltage clamp mode; ventral horn neurons were whole-cell voltage-clamped at -70mV to reveal AMPA-receptor-mediated EPSCs. The presynaptic axon was repetitively stimulated (10 stimuli at 50Hz) in a series of trains. Figure 3A shows 10 sequential responses to trains in control and in 5-HT (600nM), revealing the quantal variance in the postsynaptic response. 5-HT markedly

depressed AMPA receptor-mediated EPSCs early in the train. However, the EPSCs recover to control at the termination of the train (Figure 3B). The mean EPSC at the start of the train was consistently inhibited by 5-HT, whereas those at the end were not (Figure 3C,D). Specifically, the first EPSC was inhibited to 33 ± 6% of control in 600nM 5-HT, whereas the tenth EPSC was 88 ± 9% of control (n = 8)

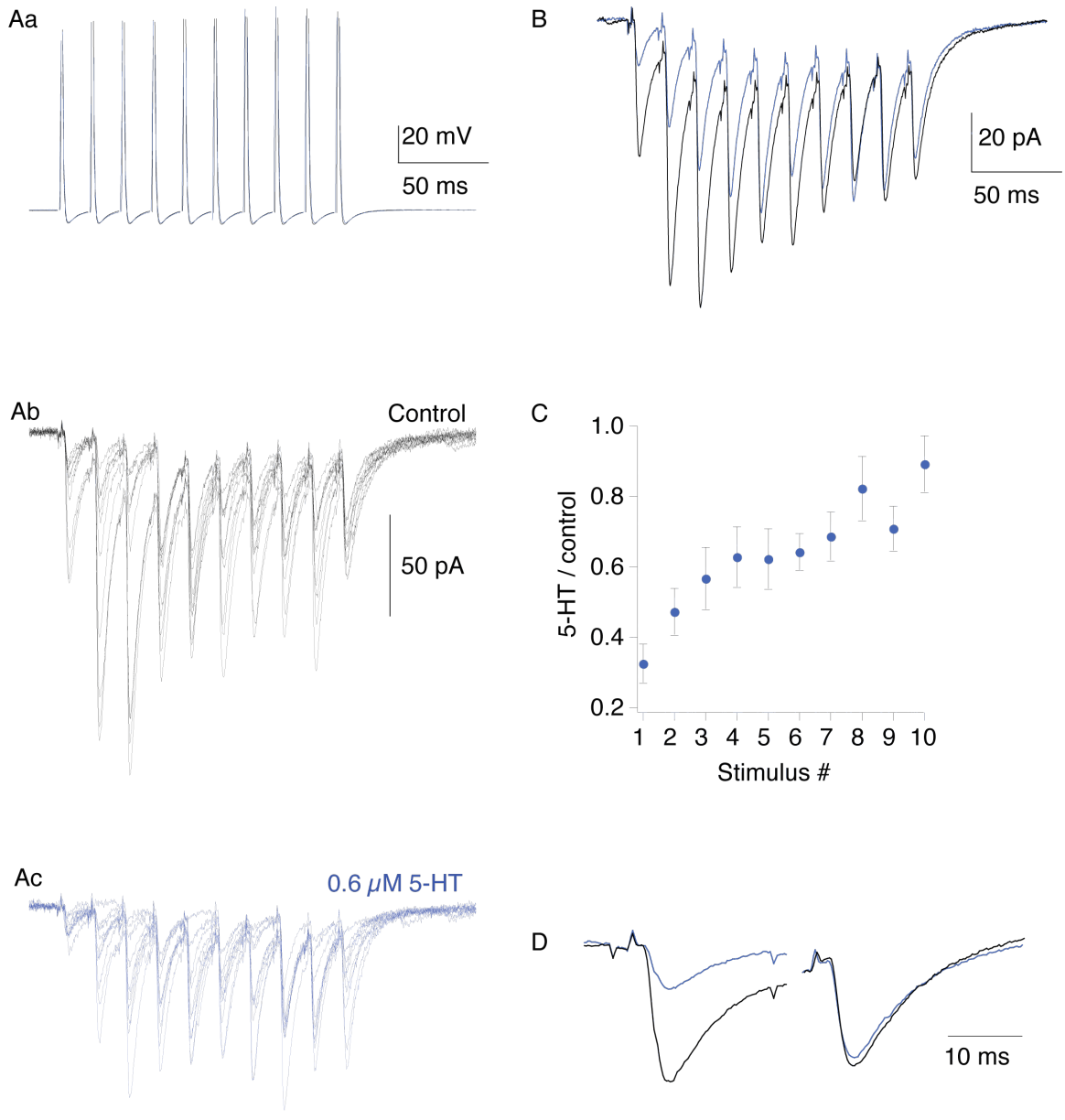
Aa
20 mV
50 ms
B
20 pA
50 ms
Ab
Control
50 pA
C
1.0
0.8
0.6
0.4
0.2
5-HT / control
1 2 3 4 5 6 7 8 9 10
Stimulus #
Ac
0.6 μM 5-HT
D
10 ms

Figure 3. 5-HT-mediated inhibition of AMPA receptor-mediated EPSCs is lost during train stimulation of the presynaptic axon. A. Paired recordings demonstrate train evoked AMPA receptor-mediated EPSCs (10 action potentials; 50 Hz in each train). Aa. Presynaptic action potentials. Ab. Ten sequential evoked EPSC trains in control and in 5-HT (Ac) (600 nM; gray). B. Means of the 10 traces shown in Ab and Ac. Control, black; 5-HT, gray. C. Ratio of EPSC amplitudes in 5-HT to control for the means of each of the 10 sequential responses in the train (n=9 preparations and pairs). 5-HT markedly inhibited the EPSCs early in the train but the response recovered toward the end. Error bars indicate SEM. D. The first and last traces are expanded and overlaid to emphasize the loss of inhibition at the end of the train.

3.2.2 Presynaptic injection of a Ca^{2+}-chelator prevents train-dependent loss of 5-HT-mediated inhibition of AMPA-receptor-mediated EPSCs

It has been shown that enhanced presynaptic Ca^{2+} transients in high extracellular Ca^{2+} prevent 5-HT1b/1d receptor-mediated presynaptic inhibition (Yoon et al., 2007b). To determine whether Ca^{2+} summation at the active zone does indeed account for the loss of 5-HT-mediated inhibition during the stimulus train as shown in Figure 3 above, frequency-dependent residual Ca^{2+} accumulation following repeated stimulation was prevented. Reticulospinal axons were recorded from as in Figure 3 above, but were microinjected with the slow-binding Ca^{2+} buffer, EGTA, to mitigate stimulation train-evoked presynaptic Ca^{2+} summation. While EGTA will reduce the slow accumulation of residual Ca^{2+} at the active zone during repetitive stimulation, it does not prevent individual evoked EPSCs because it does not bind Ca^{2+} sufficiently rapidly to prevent its immediate binding to synaptotagmin (Adler et al., 1991). EGTA was injected into the presynaptic axons (electrode contained 100mM EGTA, 5mM HEPES, 1M KCl, pH 7.2; n=5). Notably, all chemical EPSCs are inhibited by this injection (Figure 4A).

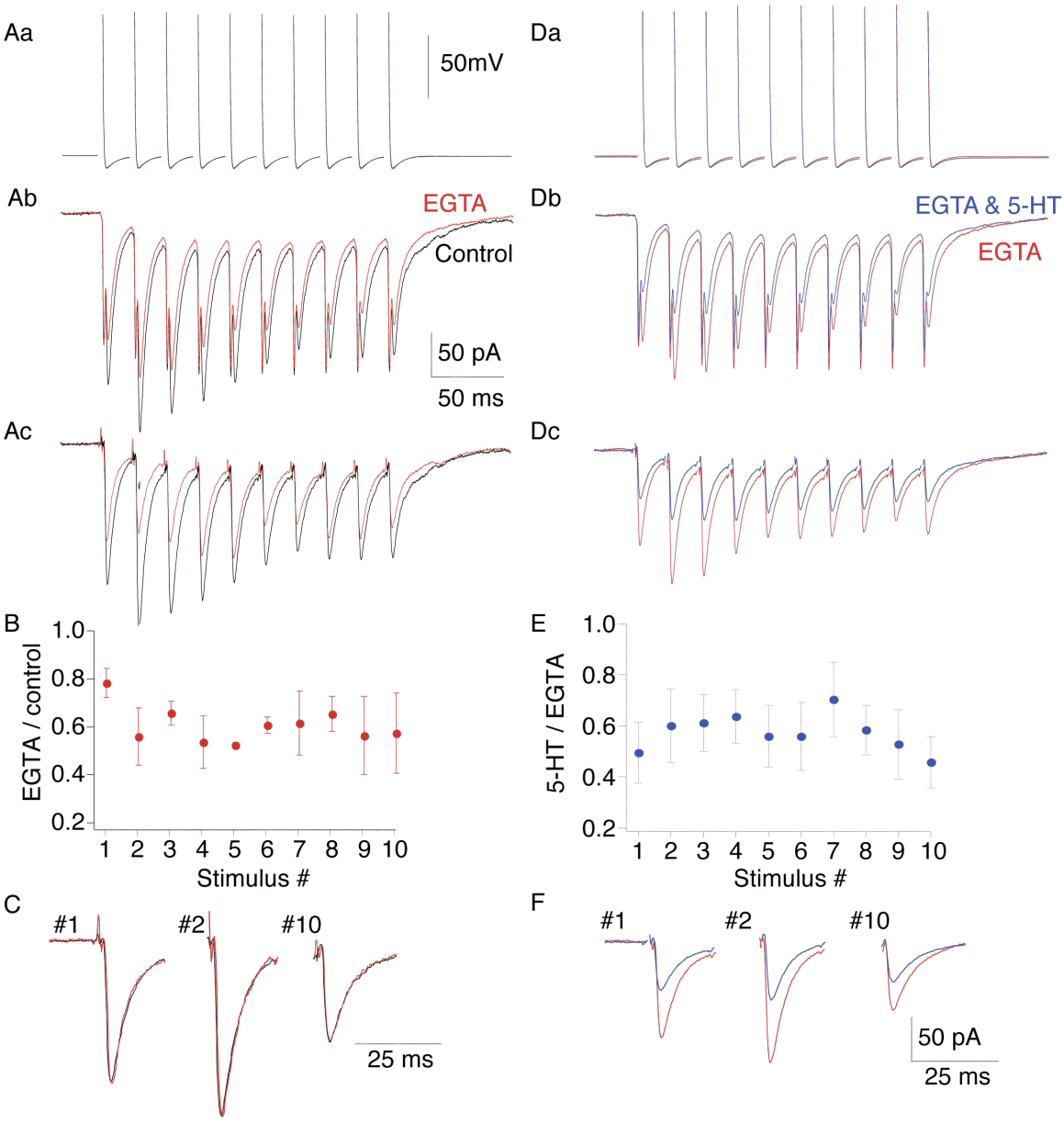
Aa
50mV
Ab
EGTA
Control
50 pA
50 ms
Ac
Da
Db
EGTA & 5-HT
EGTA
Dc
B
EGTA / control
1.0
0.8
0.6
0.4
0.2
1 2 3 4 5 6 7 8 9 10
Stimulus #
C
#1
#2
#10
25 ms
E
5-HT / EGTA
1.0
0.8
0.6
0.4
0.2
1 2 3 4 5 6 7 8 9 10
Stimulus #
F
#1
#2
#10
50 pA
25 ms

Figure 4. Train-dependent loss of 5-HT-mediated inhibition is prevented by presynaptic injection of EGTA. A, Paired recording between presynaptic reticulospinal axon and postsynaptic neuron in which EGTA (100 mM) was included in the presynaptic electrode. Aa, Presynaptic action potentials before (black) and after (red) pressure injection of EGTA into the axon. EGTA left action potentials unaffected throughout the train. Ab, Postsynaptic EPSCs comprising electrical and chemical components evoked by presynaptic action potentials. Traces are averages of 10 responses before and after injection of EGTA into the presynaptic axon. Ac, Chemical EPSCs after subtraction of the electrical components that were obtained after blocking AMPA-mediated responses with CNQX. B, Effect of EGTA injection as proportional inhibition for each of the 10 EPSCs in the train. Data are from four paired recordings and normalized to control amplitudes of each EPSC. The first response was inhibited to a lesser extent than later responses in the train. C, As representative examples, the first, second, and last EPSCs in the train were compared before and after EGTA injection. The responses after EGTA were scaled to the peak amplitudes of the control responses. The kinetics of the responses (both rise and decay) were unaltered. D, Paired recordings from cell in A; red traces are the same as those in A after presynaptic EGTA injection. Da, Presynaptic action potentials. Db, Evoked EPSCs in EGTA and 5-HT (600 nM; blue). Dc, Traces after subtraction of electrical compo- nents. E, Ratio of EPSC amplitudes in 5-HT to control (n=5 preparations and pairs). 5-HT inhibited EPSCs throughout the train after presynaptic EGTA injection. Error bars indicate SEM. F, The first, second, and last traces are expanded to emphasize that inhibition is sustained throughout the train.

However, the first response is less inhibited than the subsequent responses (mean reduction of first respone to 78 ± 6% of control, whereas mean of all later responses was 58 ± 2% of control; $p < 0.05$) (Figure 4B). The later depression of the response is common at this synapse, but the underlying mechanism remains unclear. Figure 4C illustrates that the kinetic profile of the individual responses during the stimulation train was not altered by the presynaptic injection of EGTA.

Also noteworthy is the finding that 5-HT (600nM) inhibited EPSCs uniformly throughout the presynaptic stimulus train following presynaptic injection of this Ca^{2+} chelator (Figure 4D). For example, the first response was reduced to 49 ± 12% of control, which was not significantly different from results without EGTA; the last response in the train was reduce to 43 ± 10% of control, which was not significantly different from the effect of 5-HT on the first response. (Figure 4E, F). This means that the inhibitory effect of 5-HT on late responses during presynaptic stimulus trains was significantly enhanced after presynaptic EGTA injections ($p < 0.05$). Thus, these results provide confirmation that presynaptic residual Ca^{2+} accumulates during stimulation trains and mediates a loss of 5-HT-mediated presynaptic inhibition, an effect that is consistent with Ca2+-synaptotagmin competition with Gβγ at the SNARE complex.

It is clear from these data that Ca^{2+} accumulation from repetitive stimulation can modify synaptic vesicle fusion properties in the presence of 5-HT. Consequently, for further experiments to ensure that evoked Ca^{2+} did not

accumulate during stimulus trains used to load axons with FM1-43, I chose a stimulation rate that will not allow temporal summation of the presynaptic Ca^{2+} signal. The mean decay rate (tau) of the lamprey giant axon is approximately 1s (Takahashi et al., 2001). Consequently, all synaptic vesicle loading with FM1-43 was performed at a stimulation rate of 0.5 - 1Hz.

3.2.3 Dynamin Inhibition during 5-HT-mediated presynaptic Inhibition

Axons that have been loaded with FM1-43 can be destained and reloaded under stimulation. To destain the average lamprey giant reticulospinal axons under control conditions, as few as 2000 stimuli is sufficient, while others may require a larger number of stimuli to destain due to the heterogeneity of synaptic vesicle pools in this model axon.

As shown in Figure 5, axons load FM1-43 dye and destain through stimulation. Here, in order to label the presynaptic vesicle cluster with FM1-43, 2000 action potentials were induced at 5Hz in the presence of FM1-43 (4μM), after which time excess FM1-43 was washed away and cleared with Advasep-7 (1mM) (Kay et al., 1999; Photowala et al., 2005; Bleckert et al., 2012). Baseline is defined as a stable level of fluorescence in the absence of further stimulation (time points preceding time t=0 min, Figure 5Ba). FM1-43 fluorescence decreases in response to stimulation (Figure 5A, 5Bb). Axon health is monitored via microelectrode recordings; axons whose resting membrane potential rises above -65 millivolts are discarded. Healthy axons can be reloaded utilizing the same protocol (Figure 5Bc, here 5Hz, 2000 stimuli). Thus, FM1-43 fluorescence

serves as a powerful measure of endocytosis and exocytosis at the presynaptic terminal.

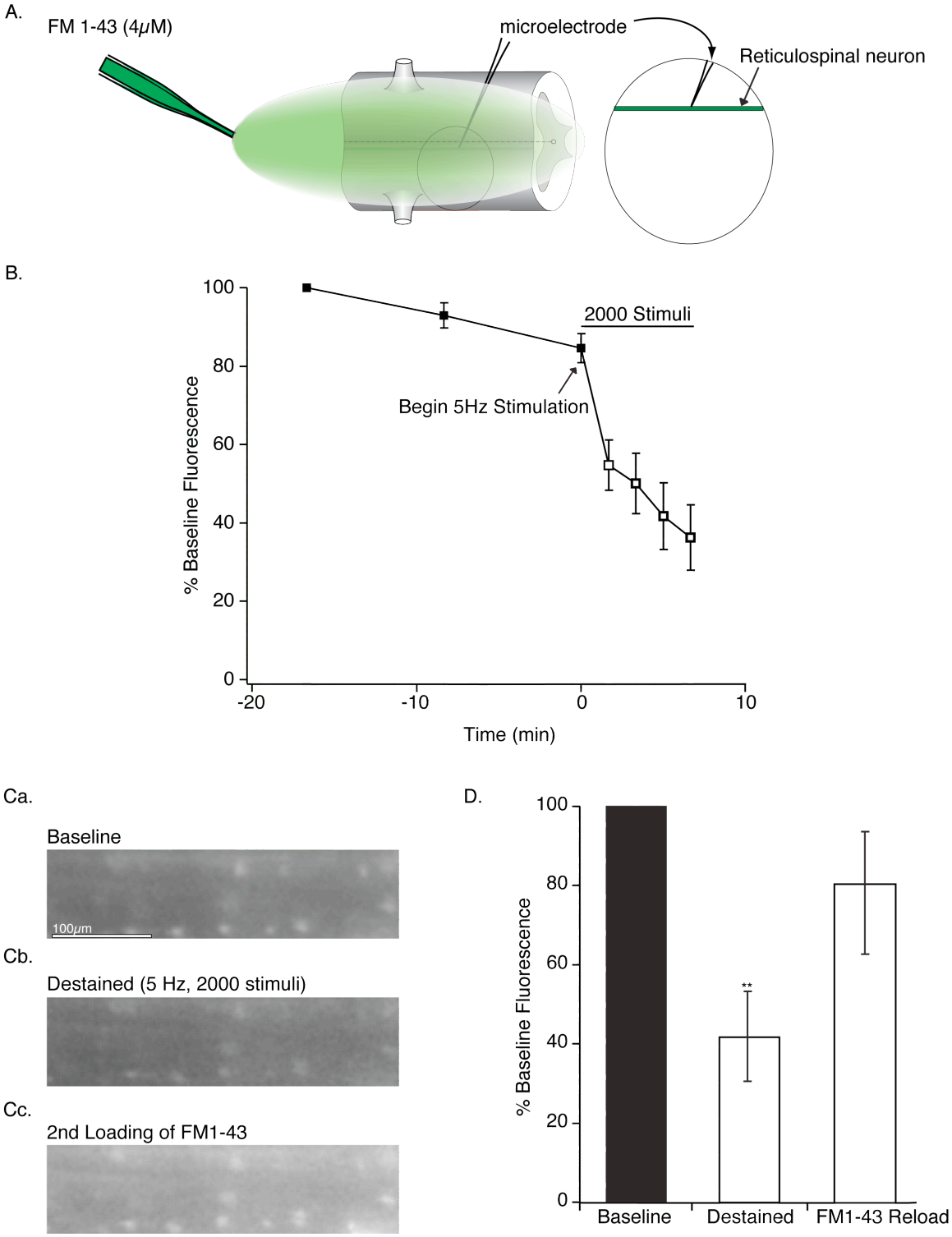
A.
FM 1-43 (4μM)
microelectrode
Reticulospinal neuron
B.
100
80
60
40
20
0
% Baseline Fluorescence
2000 Stimuli
Begin 5Hz Stimulation
-20
-10
0
10
Time (min)
Ca.
Baseline
100μm
Cb.
Destained (5 Hz, 2000 stimuli)
Cc.
2nd Loading of FM1-43
D.
100
80
60
40
20
0
% Baseline Fluorescence
**
Baseline
Destained
FM1-43 Reload

Figure 5. Control FM1-43 loading and destaining in axons. A. Schematic demonstrating flow of FM1-43 with stimulating electrode placement in reticulospinal axon on ventral surface of lamprey spinal cord preparation. B. Timecourse demonstrating stability of FM1-43 fluorescence at baseline, followed by stimulation-dependent destaining (5Hz, 2000 stimuli). Ca.-Cc. Representative micrographs showing baseline (Ca), destained (Cb), and re-loaded axons (Cc), respectively. (Inset: 100μm scale bar). D. Bar graphs illustrating significant reduction in FM1-43 fluorescence following stimulation; additional bar showing FM1-43 fluorescence rising upon second reloading. (**, $p<0.005$, Student's t-test).

In contrast, axons that have been loaded with FM1-43 do not destain under low frequency stimulation in the presence of 600nM 5-HT. This was originally demonstrated by the Alford laboratory (Photowala et al., 2006), where 5000 stimuli delivered at 1Hz failed to destain FM1-43-loaded axons in the presence of 600nM 5-HT. Using the same protocol, I was able to repeat this effect, again showing that FM1-43-loaded axons do not destain in 600nM 5-HT (Figure 6A,B). Continuing stimulation at 1Hz, dynasore (20μM) was washed in while the axons were stimulated for an additional 5000 stimuli (10,000 total stimuli). 5-HT-mediated inhibition of FM1-43 destaining is clearly inhibited when dynamin is blocked via dynasore (20μM) (Figure 6A,B). Whereas FM1-43-loaded axons destained to 70.2 ± 16.2% of baseline fluorescence in the presence of 600nM 5-HT (5000 stimuli, 1Hz; not significantly different from control FM1-43 staining over a similar period of recording but with no applied stimuli (Bleckert et al., 2012)), upon exposure to 20μM dynasore, these same axons destained to 37.0 ± 7.3% of baseline fluorescence ($p < 0.05$, Student's t-test).

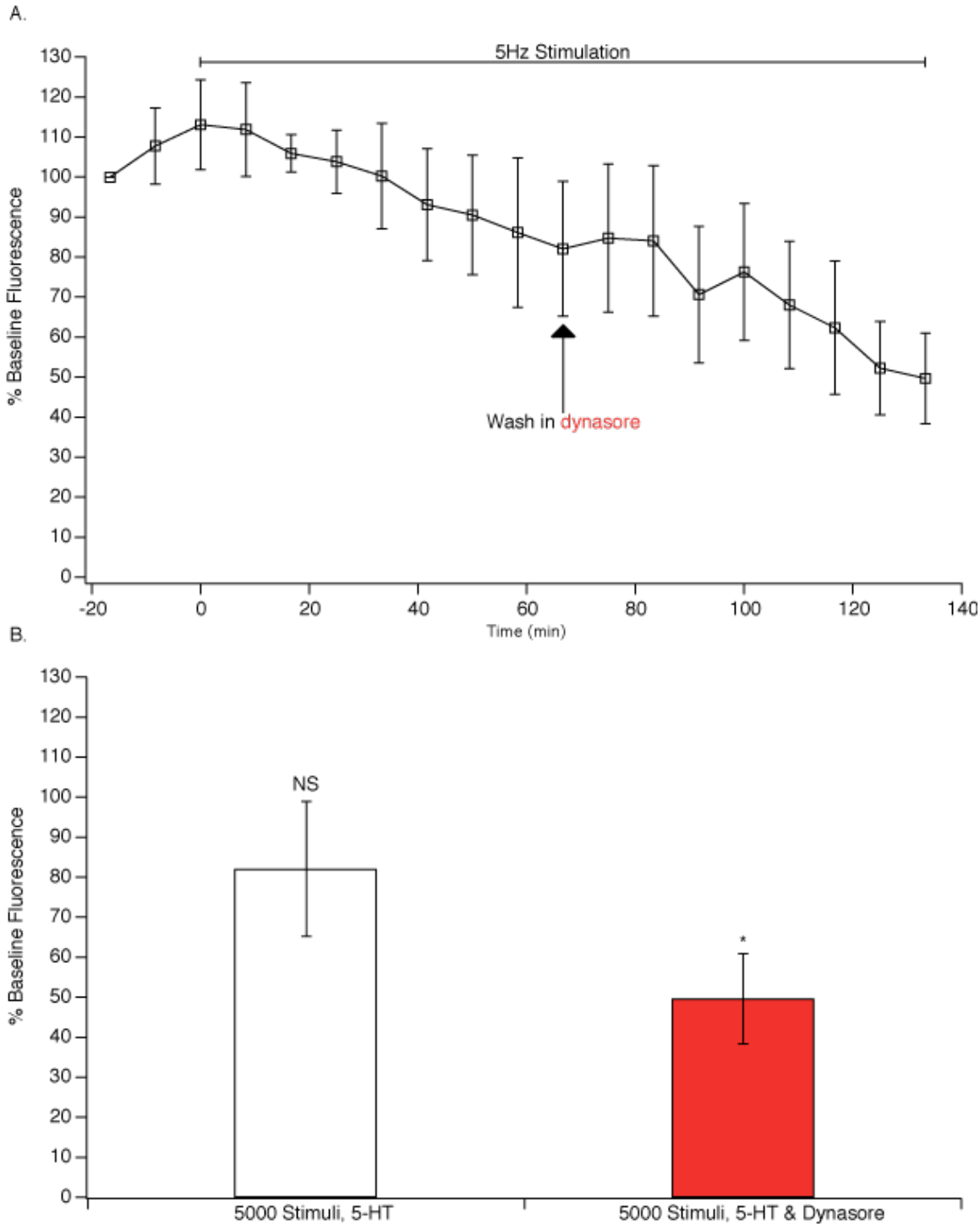
A.
5Hz Stimulation
% Baseline Fluorescence
Wash in dynasore
Time (min)
B.
% Baseline Fluorescence
NS
*
5000 Stimuli, 5-HT
5000 Stimuli, 5-HT & Dynasore

Figure 6. Dynasore relieves inhibition of FM1-43 destaining in the presence of 5-HT. A. FM1-43 fluorescence was more stable under 1Hz stimulation in the presence of 600nM 5-HT (5000 stimuli) than when 20μM dynasore was applied in addition to 5-HT (same cells, 5000 stimuli). B. Bar graphs demonstrating greater FM1-43 destaining (mean ± SEM of fluorescence values after 5000 stimuli expressed as % of baseline) in dynasore and 5-HT versus 5-HT alone (*, $p < 0.05$; **, $p < 0.005$, Student's t-test).

As the schematic in Figure 7A illustrates, under control destaining conditions, FM1-43-loaded vesicles fully fuse with the presynaptic membrane, exposing membrane-embedded FM1-43 to the aqueous environment of the synaptic cleft, where it dissipates almost completely. In contrast, in the presence of 5-HT, the mode vesicle fusion is switched from full to kiss-and-run, and thus, FM1-43 dye embedded in the membrane of the vesicle lumen does not escape (Figure 7B). I propose a mechanism in Figure 7C to explain how 5-HT-mediated inhibition of FM1-43 destaining is relieved when dynamin is inhibited via dynasore. In this case, I believe the fusion pore is retained in an open configuration after the vesicle "kisses" the presynaptic membrane, allowing a prolonged access to the aqueous environment of the synaptic cleft. As such, FM1-43 that has dissociated from the membrane of the vesicle lumen, can escape through the fusion pore. I hypothesized that dynamin inhibition would relieve inhibition of FM1-43 destaining in 5-HT, which is supported by the above data. I believe this suggests that dynamin is involved in kiss-and-run fusion, which has not been previously shown in the literature.

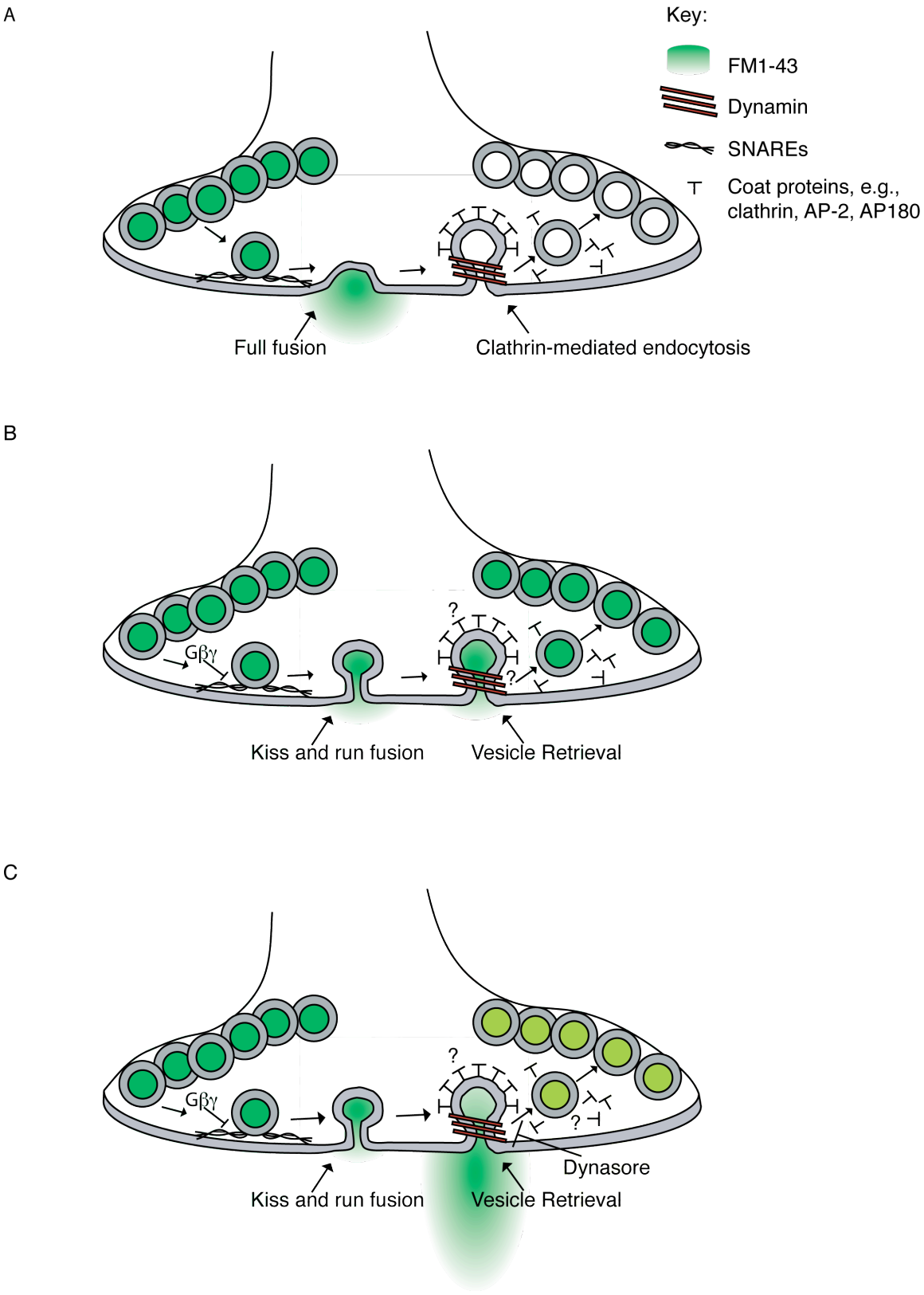
A
Key:
FM1-43
Dynamin
SNAREs
Coat proteins, e.g., clathrin, AP-2, AP180
Full fusion
Clathrin-mediated endocytosis
B
Gβγ
?
?
Kiss and run fusion
Vesicle Retrieval
C
Gβγ
?
?
Dynasore
Kiss and run fusion
Vesicle Retrieval

Figure 7. Schematics illustrating proposed mechanisms behind FM1-43 destaining in control conditions and in the presence of 5-HT and dynasore. A. Control FM1-43 destaining. B. FM1-43 destaining in the presence of 5-HT. C. FM1-43 destaining in the presence of 5-HT and dynasore. Question marks are used to show that some players of clathrin-mediated endocytosis, e.g., coat proteins and dynamin, remain to be determined as factors in vesicle retrieval under kiss-and-run conditions.

As discussed above, FM1-43 loading is possible in 600nM 5-HT, albeit to a lesser extent than under control conditions (Photowala et al., 2006). However, based on the notion of a retained fusion pore illustrated in Figure 7C, loading of FM1-43 in the presence of 5-HT (600nM) and dynasore (20μM) should be completely abolished if dynamin is required for endocytosis under these conditions. However, in the presence of dynasore (20μM) and 5-HT (600nM), it was clearly possible to load synaptic vesicles with FM1-43 (Figure 8). Loading was similar in absolute fluorescence values (signal bit depth in puncta within individual presynaptic terminals, subtracting background bit depth). This is true for comparison with the two control experiments here, but also in data published in Photowala et al (2006).

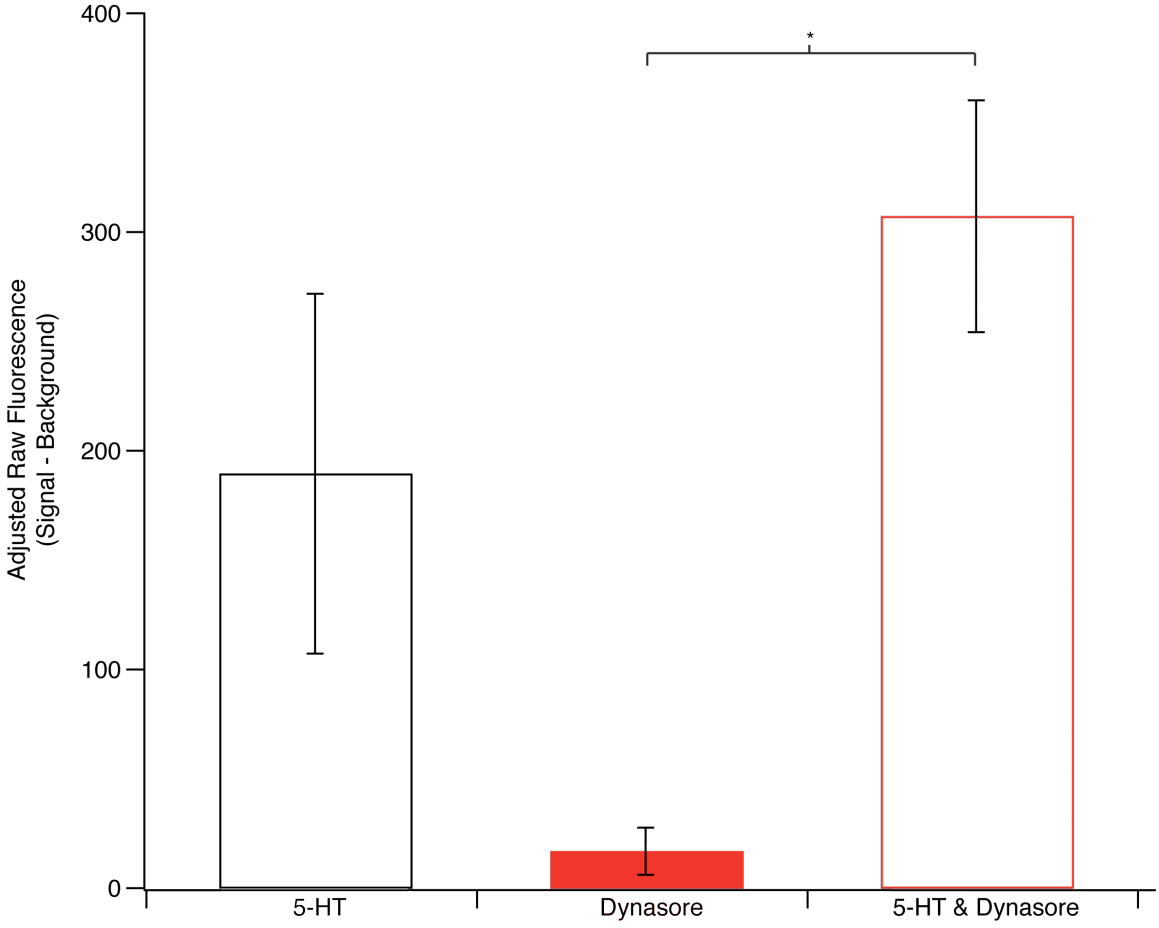
400
300
200
100
0
Adjusted Raw Fluorescence
(Signal - Background)
*
5-HT
Dynasore
5-HT & Dynasore

Figure 8. Dynasore has no effect on FM1-43 loading in 5-HT. A. Mean adjusted raw fluorescence from axons loaded with FM1-43 in the presence of 5-HT (600nM; 0.5Hz, 1000 stimuli; black open box; n = 2); in the presence of dynasore (20µM; 5Hz, 2000 stimuli; red filled box; n = 4); and in the presence of 5-HT (600nM) and dynasore (20µM) (0.5Hz, 1000 stimuli; red open box; n = 4). (Mean ± SEM; *, $p < 0.05$; Student's t-test).

As the schematic in Figure 9A illustrates, loading of FM1-43 in the presence of 5-HT is possible, as shown by Photowala et al (2006). In contrast, when CME is blocked by inhibition of dynamin, e.g., by dynasore or DIP (see also Figure 15), loading of FM1-43 is almost completely abolished (Figure 8, and schematic in Figure 9B). Because FM1-43 loading was still evident under kiss-and-run conditions in 5-HT when dynamin was blocked, it appears dynamin is not involved in kiss-and-run fusion, as illustrated in Figure 9C. It is still unclear whether other components of CME, e.g., coat proteins, as shown in Figure 9C.

A

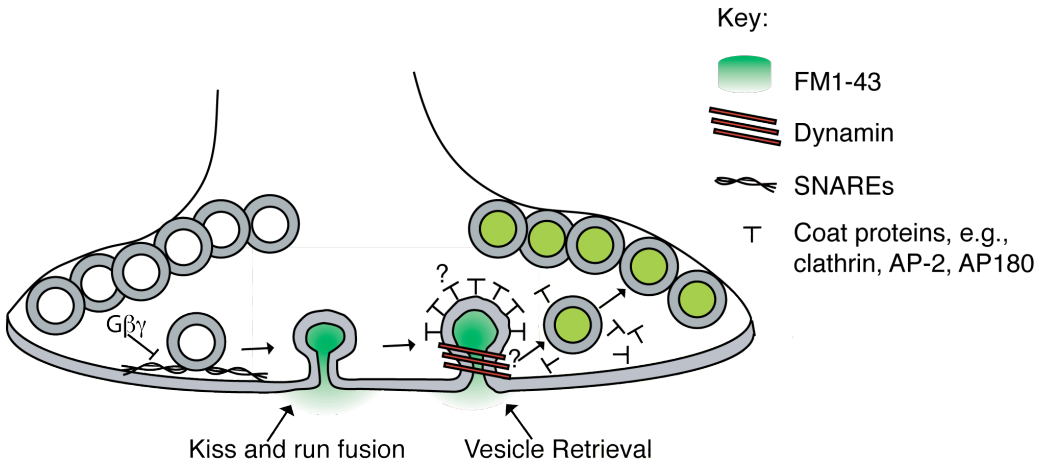
Key:
FM1-43
Dynamin
SNAREs
Coat proteins, e.g., clathrin, AP-2, AP180
Gβγ
?
?
Kiss and run fusion
Vesicle Retrieval

B

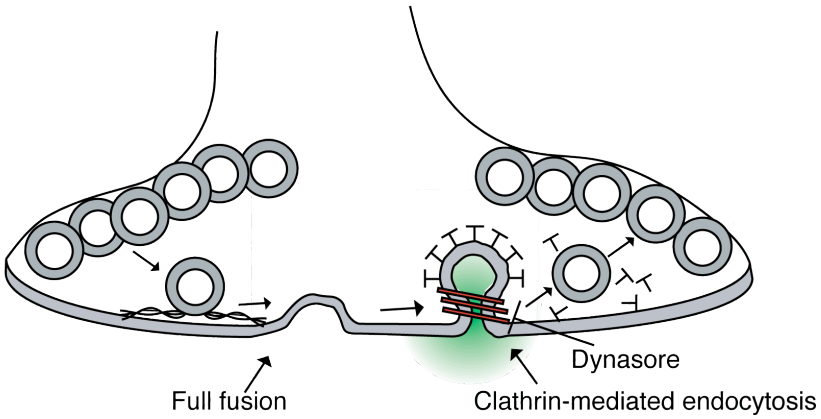
Dynasore
Full fusion
Clathrin-mediated endocytosis

C

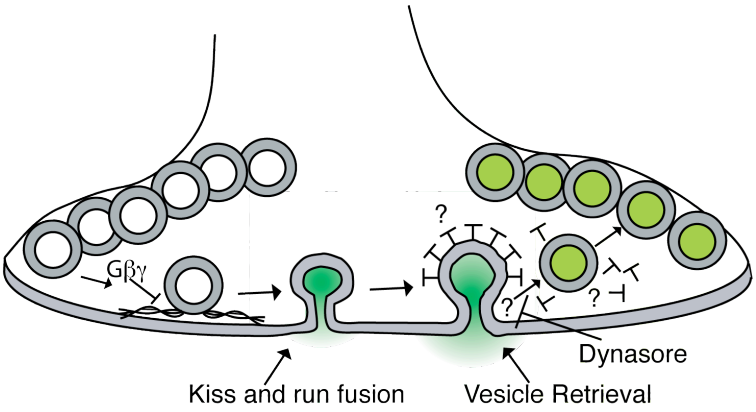
Gβγ
?
?
?
Dynasore
Kiss and run fusion
Vesicle Retrieval

Figure 9. Schematics illustrating proposed mechanisms behind FM1-43 destaining in control conditions and in the presence of 5-HT and dynasore. A. Partial FM1-43 loading in 5-HT. B. Inhibition of FM1-43 loading presence of dynasore. C. No inhibition of partial FM1-43 loading in the presence of 5-HT and dynasore.

3.3 Discussion

5-HT-mediated presynaptic inhibition is clearly dependent on the frequency of stimulation. Following the last action potentials of high frequency stimulation trains (10 action potentials at 20Hz), this inhibition was prevented (Figure 3). Furthermore, presynaptic injection of a slow-binding Ca^{2+} chelator allowed a uniform 5-HT-mediated presynaptic inhibition, by preventing frequency-dependent residual presynaptic Ca^{2+} summation (Figure 4). This provided a rationale for using low-frequency stimulation as a means of initiating compensatory exocytosis in the presence of 5-HT. Furthermore, it ensured that kiss-and-run was the predominant mode of vesicle fusion, as higher frequency stimulation switches the vesicle fusion mode to full fusion *(*Harata et al*.,* 2006a*)*.

It remains paradoxical that dynamin inhibition prevents presynaptic 5-HT-mediated blockade of FM1-43 destaining, yet has no effect on FM1-43 loading in the presence of 5-HT. It is possible that this may be due to the presence of multiple vesicle fusion modes simultaneously occurring, that is, some engaging in full fusion and/or clathrin-mediated endocytosis and others engaging in kiss-and-run. Thus, perhaps Gβγ may not have uniform access to all lamprey giant reticulospinal presynaptic SNAREs. In this hypothesized condition, either separate pools of vesicles previously loaded with FM1-43 under control conditions, or separate pools of vesicles being loaded with FM1-43 in the presence of 5-HT, could be differentially affected by dynamin inhibition. Alternatively, if a dynamin-dependent retained fusion pore is responsible for

enhanced FM1-43 destaining in the presence of 5-HT (Figure 7C), it is possible that dynamin inhibition might alleviate tethering of these vesicles to cytoskeletal structures, e.g., actin *(Galletta and Cooper, 2009; Galletta et al., 2010)*, allowing a greater number of them to fuse with the presynaptic membrane than would be possible in 5-HT alone. Finally, it is possble that the effect of the inhibition of dynamin on already stained vesicles in the presence of 5-HT is not directly related to fusion properties of the vesicles at all. Rather, I hypothesized that dynamin plays a role in the the stabilty of the stained vesicle cluster in the presence of 5-HT rather than modifying the properties of fused vesicle and their endocytotic fate. Clearly, dynamin inhibition has no effect on FM1-43 loading in the presence of 5-HT, which suggests that dynamin is not required in endocytosis of FM1-43 stained vesicles following kiss-and-run fusion (Figure 8). As the next chapter illustrates, dynamin inhibition has a potent effect on nerve terminals at rest, which may explain this paradoxical effect.

4. DYNAMIN IS NECESSARY FOR MAINTENANCE OF VESICLE POOLS IN RESTING PRESYNAPTIC TERMINALS

4.1 Introduction

Vesicle pools in cells are maintained by a variety of mechanisms, dependent upon protein-protein interactions, including those with the cytoskeleton, as well as endocytic *(Bähler and Greengard, 1987; Gitler et al., 2008; Galletta and Cooper, 2009; Yamada et al., 2009; Galletta et al., 2010; Taylor et al., 2012)* and exocytic protein interactions *(Neale et al., 1999; Graham et al., 2000; Archer et al., 2002)*. In a resting presynaptic terminal, the maintenance of pools of vesicles critically depends on the regulation of these proteins, as perturbations can change the size of the vesicle pools *(Ferguson et al., 2009; Bykhovskaia, 2011)*, altering neurotransmission *(Delgado et al., 2000; Xue and Mei, 2011)*.

Based on the overwhelming evidence for the intimate relationship of dynamin to the vesicle cycle *(Hinshaw and Schmid, 1995; Shupliakov et al., 1997; Smillie and Cousin, 2005; Yoshida and Takei, 2005; Macia et al., 2006; Newton et al., 2006; Lu et al., 2009; Douthitt et al., 2011; Schmid and Frolov, 2011)*, it is known that dynamin inhibition is a potent means of inhibiting CME. Dominant negative mutants of dynamin isoforms have yieled interesting results, showing altered regulation of proteins that interact with dynamin in interesting ways *(Lou et al., 2012)*. However, fundamental control experiments examining the effects of acute inhibition of dynamin in resting presynaptic terminals are lacking. Thus, I was interested in determining what happens when dynamin is inhibited in resting presynaptic terminals.

4.2 Results

4.2.1 Dynamin inhibition diminishes FM1-43 fluorescence at rest

Following loading via standard protocol, FM1-43 fluorescence is stable across time in the absence of stimulation when the preparation is continuously superfused with fresh lamprey Ringer (Figure 10A,B) (see also (Bleckert et al., 2012). However upon exposure to the cell-permeable dynamin-1 and -2 GTPase inhibitor dynasore (20μM), FM1-43 fluorescence of previously stained synaptic vesicle clusters decreases, reaching a plateau level of about 40% of control (Figure 10B). Exposing tissue to the identical final concentration (0.00375%) of dimethyl sulfoxide (DMSO), the medium in which dynasore was dissolved, yielded no change in fluorescence in tissue at rest. This rules out DMSO as a possible factor in these changes in fluorescence. Thus, inhibiting dynamin appears to mediate a change in FM1-43 fluorescence despite the lack of electrophysiological stimulation that is typically used to drive a large number of vesicles to fuse and destain. This suggests a role for dynamin in maintaining vesicle pools in cells at rest.

However, because little is known yet about the precise mechanism by which dynasore inhibits the GTPase dynamin, we repeated the above experiment with a 10-amino-acid dynamin inhibitory peptide (DIP) targeting one of dynamin's binding partners, amphiphysin. As before, we demonstrate control FM1-43 loading and stability at rest. As shown in Figure 10B, following DIP injection, FM1-43 fluorescence decreases to 54.4 ± 10.3% of baseline fluorescence. Thus,

similar to our observations with dynasore, DIP also induces a decrease in FM1-43 fluorescence in tissue at rest.

A

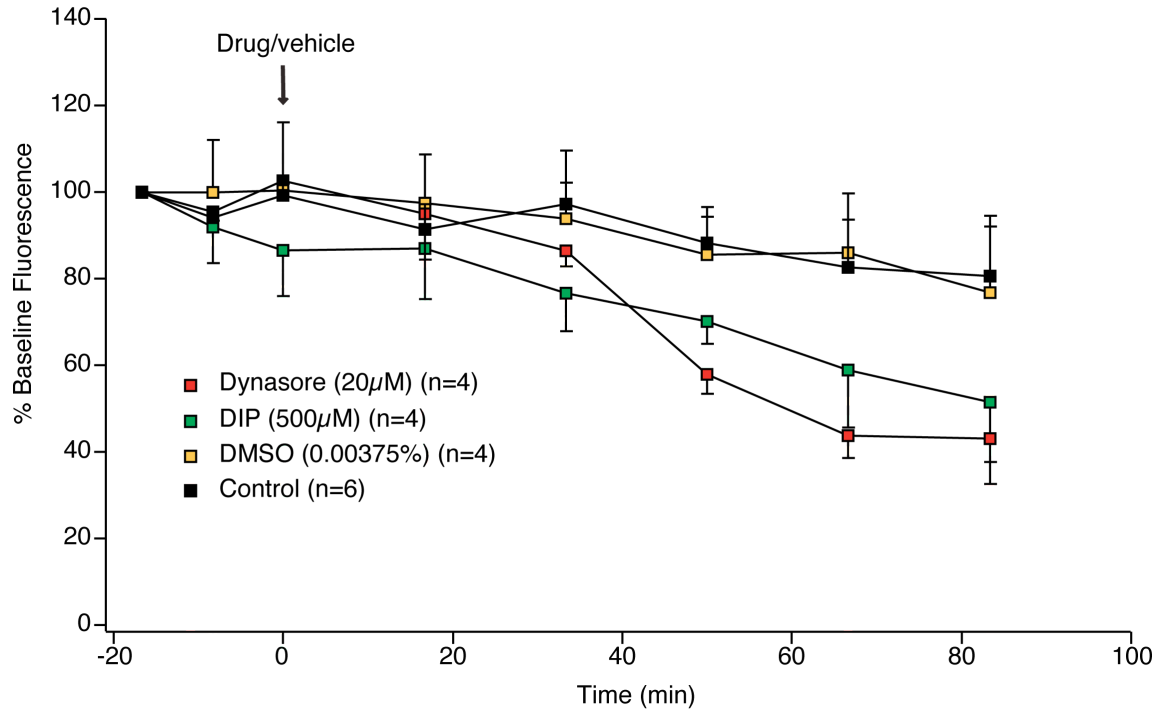
Drug/vehicle
% Baseline Fluorescence
Time (min)
Dynasore (20μM) (n=4)
DIP (500μM) (n=4)
DMSO (0.00375%) (n=4)
Control (n=6)

B

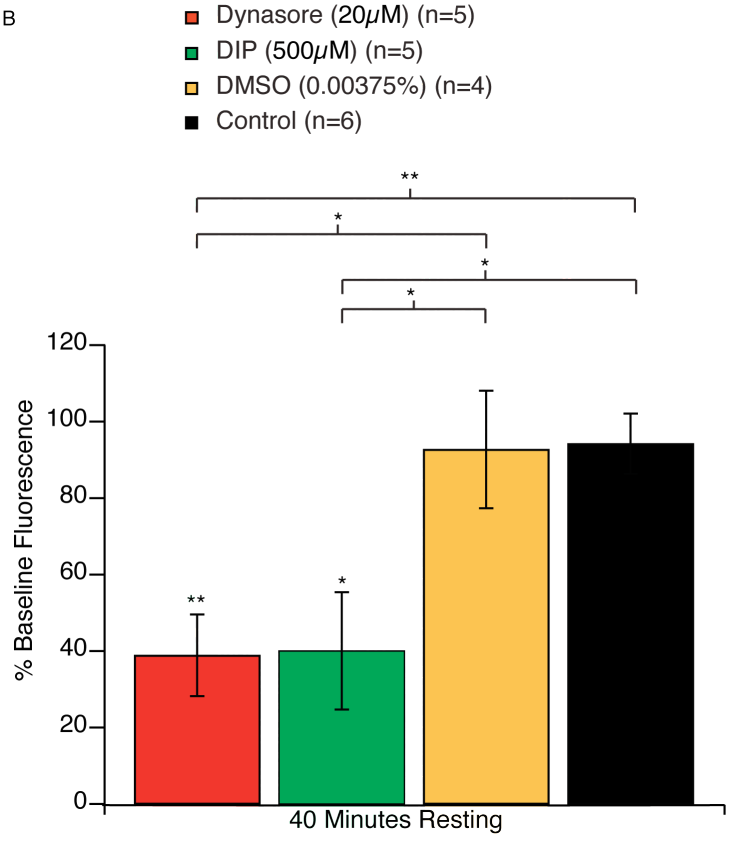
Dynasore (20μM) (n=5)
DIP (500μM) (n=5)
DMSO (0.00375%) (n=4)
Control (n=6)
% Baseline Fluorescence
40 Minutes Resting

Figure 10. Dynamin inhibition causes spontaneous loss of FM1-43 fluorescence in axons at rest. A. Axons were loaded with FM1-43, and after establishing a stable baseline, were either administered drugs targeted against dynamin isoforms 1 and 2 (dynasore, red; or dynamin inhibitory peptide (DIP), green) or observed over time in the presence of no drugs (black) or a control medium (DMSO, yellow). Following baseline measures, each data point represents the average of two fluorescence measurements spaced 500 seconds apart. Error bars represent standard error of the mean. B. Quantification of fluorescence following dynamin inhibition, showing a significant loss of fluorescence relative to baseline and controls at 40 minutes following dynamin inhibition. (*, $p<0.05$; **, $p<0.005$, Student's t-test).

DIP is derived from the proline-rich-domain (PRD) of dynamin, which is known to bind with the Src-homology (SH3) domain of amphiphysin (Schiavo et al., 1997; Shupliakov et al., 1997; Wigge and McMahon, 1998; Neale et al., 1999; Koticha et al., 2002; Verderio et al., 2004; Blackmer et al., 2005; Gerachshenko et al., 2005; Yoshida and Takei, 2005; Jörntell and Hansel, 2006; Verderio et al., 2006; Yoon et al., 2007b; Chen and Barbieri, 2011; Zhang et al., 2011; Wang et al., 2012). Consistent with work using peptides derived from SH3 domains of other dynamin-binding partners, DIP inhibits endocytosis by sequestering amphiphysin, a protein known to be crucial in endocytosis (Shupliakov et al., 1997; Wigge and McMahon, 1998; Yoshida and Takei, 2005). As early as forty minutes after pressure-injection of DIP, FM1-43 fluorescence was reduced by a similar amount to that seen following exposure to dynasore (Figure 10B). This evidence suggests that the result seen with dynasore is not due to effects on other GTPases, and is specific to dynamin, as well as a known binding partner.

4.2.2 Dynamin Inhibition does not alter spontaneous release

The Alford laboratory has previously shown stimulus dependent depletion of FM1-43 fluorescence via microelectrode stimulation (Photowala et al., 2006). This depletion of FM1-43 fluorescence is a result of FM1-43-loaded vesicles fusing with the presynaptic membrane during exocytosis, exposing membrane-embedded FM1-43 to the extracellular milieu of the synaptic cleft where it dissipates in intensity as the vesicular membrane replenishes presynaptic membrane and membrane-embedded FM1-43 subsequently washes away. To

determine whether dynasore causes spontaneous vesicle fusion, whole-cell patch recordings were performed while dynasore was washed onto the preparation (Figure 11A). The tissue was treated with TTX (1μM) to prevent evoked neurotransmitter release. Following collection of control data, dynasore (20μM) was bath-applied for up to 20 minutes. No change in frequency (11Ca, 11Cb) or amplitude (Figure 11Da, 11Db) of spontaneous mini-EPSCs was detected during this period, suggesting that dynasore did not cause vesicular exocytosis because it had no impact on spontaneous activity.

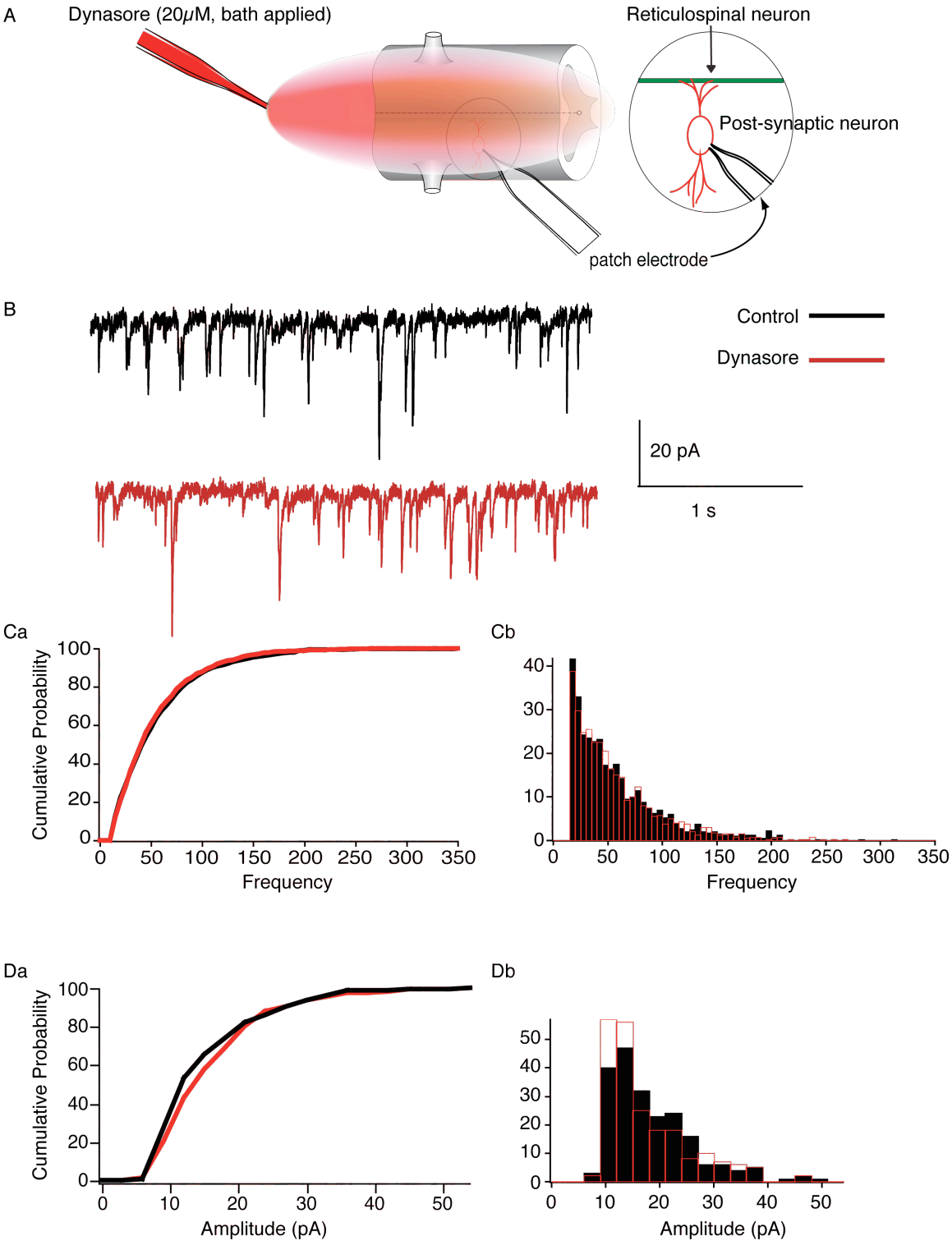
A
Dynasore (20μM, bath applied)
Reticulospinal neuron
Post-synaptic neuron
patch electrode
B
Control
Dynasore
20 pA
1 s
Ca
Cumulative Probability
Frequency
Cb
Frequency
Da
Cumulative Probability
Amplitude (pA)
Db
Amplitude (pA)

Figure 11. Dynasore does not cause changes in spontaneous glutamate release. Whole-cell patch clamp recordings were performed under control (black) and after application of dynasore (red) (n=4), and spontaneous miniature-excitatory post-synaptic currents (mEPSCs) were quantified for frequency and amplitude. A. Schematic illustrating flow of dynasore (20μM) and placement of patch electrode on post-synaptic spinal neuron (red); reticulospinal neuron appears in green. B. Traces from patched spinal neuron under control (black) conditions, and in the presence of Dynasore (red). Ca, Da. Cumulative probability plots for frequency, amplitude, respectively. Cb, Db. Histograms for frequency, amplitude, respectively.

4.2.3 Dynasore reduces vesicle pool size and alters vesicular ultrastructure in resting reticulospinal axons

As a result of my finding that dynamin inhibition causes a spontaneous loss of FM1-43 fluorescence in resting axons (Figure 10), which is independent of neurotransmitter release as shown in my analysis of mini-EPSCs following exposure to dynasore in resting axons (Figure 11), I decided to investigate whether vesicle pools changed at the ultrastructural level. Specifically, we wished to determine whether vesicle pools might be changed as a result of dynasore application. We recruited Jennifer Morgan (Assistant Scientist, Marine Biological Laboratory, Woods Hole, MA) and Andrea Foldes (currently at University of Texas Health Sciences Center, San Antonio, TX).

Dr. Morgan graciously assisted us by providing electron microscopic studies utilizing the same basic protocol we had applied. Specifically, dynasore (20μM) was applied for 30 minutes to resting lamprey giant reticulospinal axons, at which time the axons were fixed and prepared for electron microscopy. Her team was able to show that the number of vesicles at active zones was significantly reduced ($p<0.05$, Student's t-test). In addition, it appears that synaptic vesicle clusters migrated away from the synapse (Figure 12B, C). In some synapses, synaptic vesicle clusters nearly disappeared (Figure 12D).

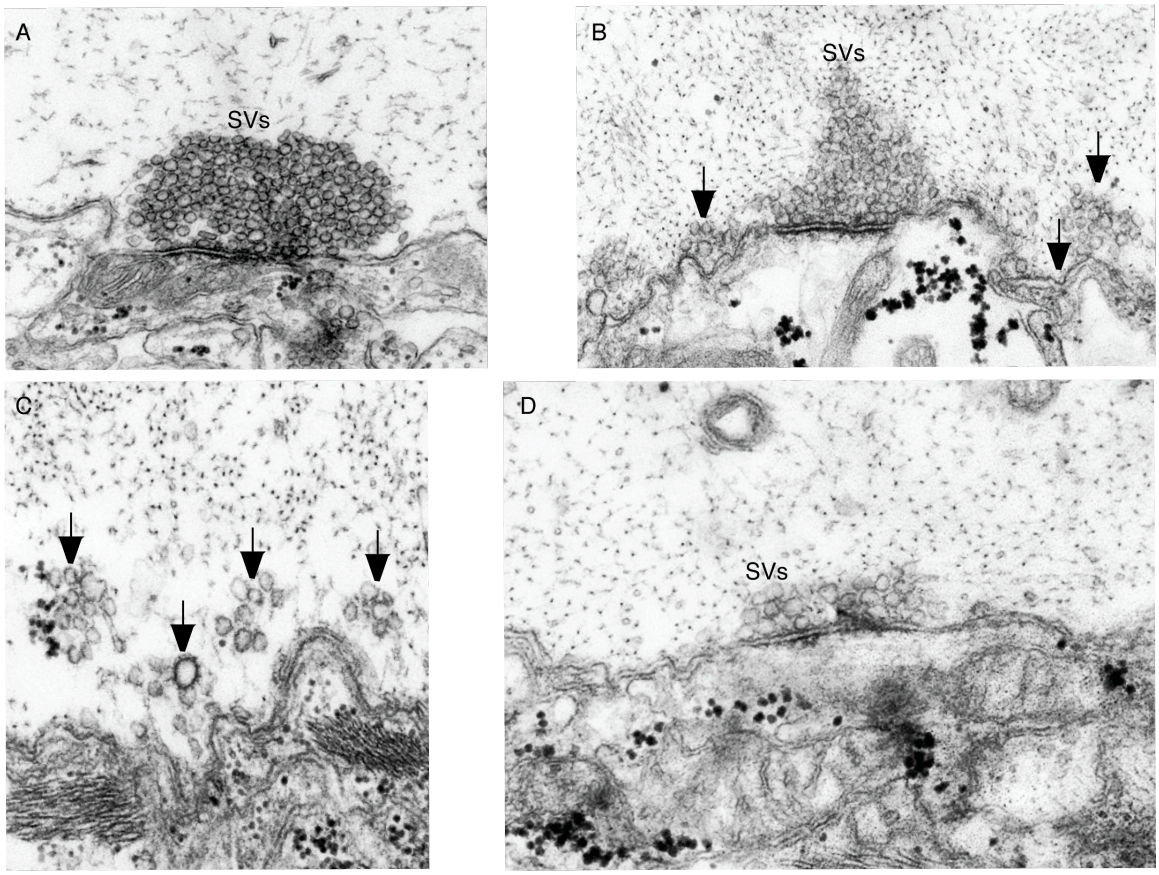
A
SVs
B
SVs
C
D
SVs

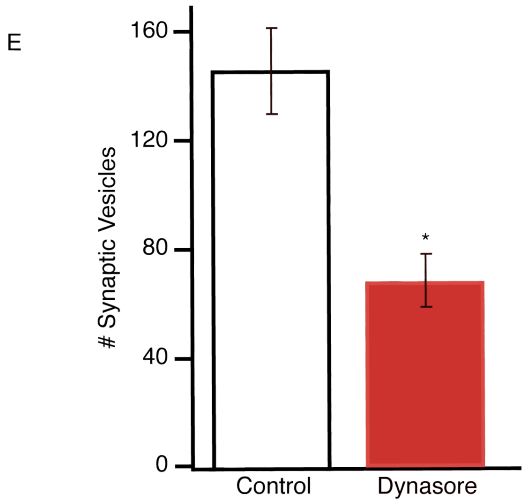
E
160
120
80
40
0
Synaptic Vesicles
*
Control
Dynasore

Figure 12. Dynasore disrupts the integrity of the vesicle cluster. A. Control giant reticulospinal synapse with large synaptic vesicle (SVs) cluster. B-D. After 30 minutes in dynasore (20μM), SV clusters are disrupted (B), disperse away from synapse (arrows in B and C), and at some synapses, are nearly absent (D). E. Quantification SV number in control and dynasore conditions, showing a significant reduction in size of SV clusters after dynasore treatment. Error bars represent +/- SEM for 10-13 synapses (*, $p < 0.05$, Student's t-test).

4.2.4 Botulinum neurotoxin B light chain blocks exocytosis

The botulinum toxins have been shown to potently block neurotransmission as a result of cleaving SNARE proteins (Schiavo et al., 1997; Neale et al., 1999; Koticha et al., 2002; Verderio et al., 2004; Blackmer et al., 2005; Gerachshenko et al., 2005; Jörntell and Hansel, 2006; Verderio et al., 2006; Yoon et al., 2007b; Chen and Barbieri, 2011; Zhang et al., 2011; Wang et al., 2012). Botulinum neurotoxin B (BoNT B), which blocks exocytosis by cleaving synaptobrevin/VAMP-1 (Schiavo et al., 1992; Shupliakov et al., 1997; Wigge and McMahon, 1998; Yoshida and Takei, 2005), was chosen to test whether loss of vesicle cluster FM1-43 fluorescence was mediated by exocytosis, or whether this destaining could occur in the absence of exocytosis. Following presynaptic microinjection of BoNT B, as few as 310 action potentials depletes the readily releasable pool of vesicles (Shupliakov et al., 1997; Wigge and McMahon, 1998; Gerachshenko et al., 2005; Yoshida and Takei, 2005). Specifically, excitatory post-synaptic currents were indistinguishable from noise following 310 action potentials delivered at a frequency of 1 Hz. We were able to replicate this result using FM1-43 fluorescence as a proxy for exocytosis, as shown in Figure 11. A small percentage of vesicles will be exocytosed following BoNT B microinjection because BoNT B cannot cleave synaptobrevin in vesicles that have already been primed; in contrast, synaptobrevin present on all unprimed vesicles is accessible to BoNT B (Gerachshenko et al., 2005; Photowala et al., 2006). After demonstrating a stable baseline level of

fluorescence in selected ROIs, BoNT B was microinjected into the respective axon at a region distal to the ROI (Figure 13), and a stimulation train was then applied (5Hz, 2000 stimuli). Similar to the effect on EPSC amplitude, this stimulation train (note this is well above 310 action potentials) decreased FM1-43 fluorescence to 82.4 ± 4.5% of baseline fluorescence ($n=9$, $p<0.05$, Student's t-test), after which fluorescence remained unchanged upon further stimulation.

A

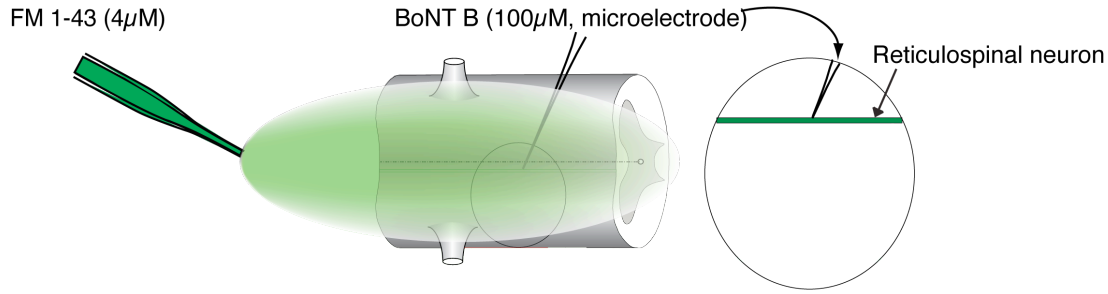
FM 1-43 (4μM)
BoNT B (100μM, microelectrode)
Reticulospinal neuron

B

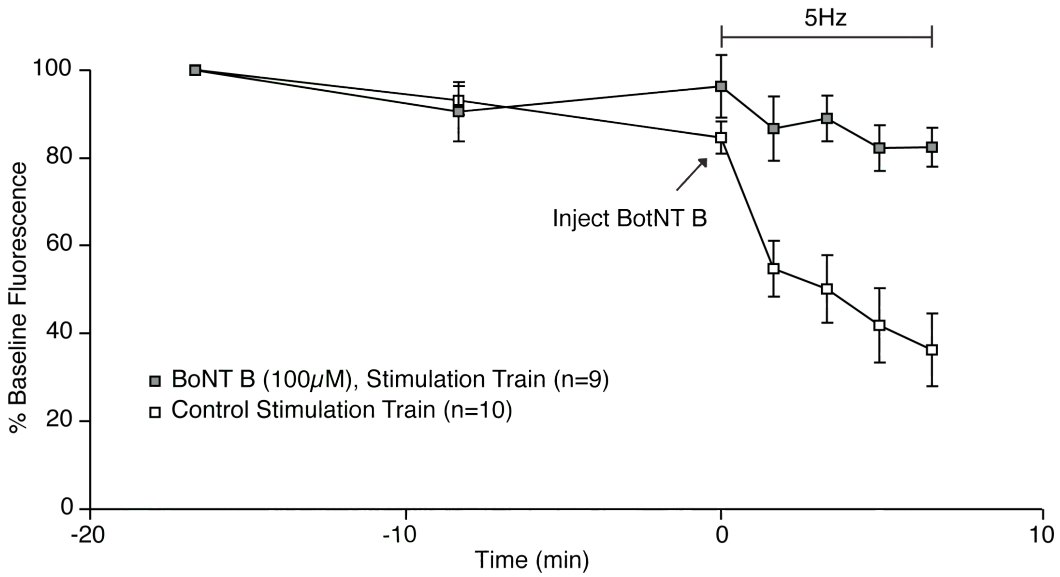
5Hz
100
80
60
40
20
0
% Baseline Fluorescence
Inject BotNT B
BoNT B (100μM), Stimulation Train (n=9)
Control Stimulation Train (n=10)
-20
-10
0
10
Time (min)

C

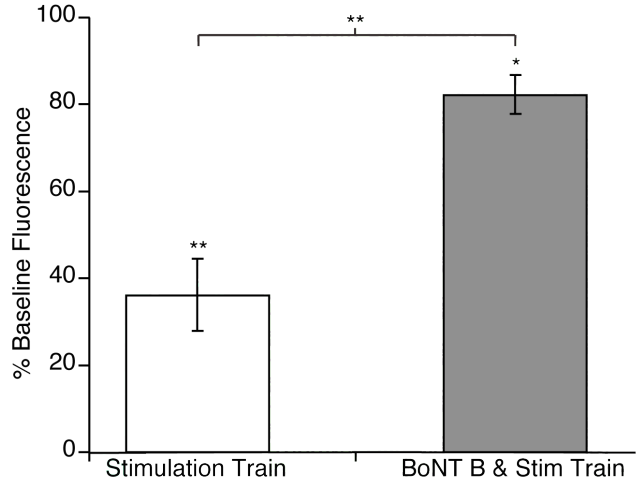
100
80
60
40
20
0
% Baseline Fluorescence
**
*
**
Stimulation Train
BoNT B & Stim Train

Figure 13. Botulinum neurotoxin B light chain (BoNT B) abolishes exocytosis. A. Schematic demonstrating FM1-43 staining protocol and BoNT B microinjection. B. Following demonstration of stability of fluorescence at rest/baseline (black, n=19), FM1-43 fluorescence decreases in a stimulation dependent manner (white) (n=10). BoNT B microinjection abolishes this stimulation dependent FM1-43 destaining (n=9). C. Bar graph demonstrating that BoNT B abolishes exocytosis. Specifically, whereas control FM1-43 destaining resulted in a decrease to 36.2 ± 8.3% of baseline fluorescence (**, $p<0.005$, Student's t-test), FM1-43 destaining following BoNT B microinjection resulted in a decrease to 82.4 ± 4.5% of baseline fluorescence (*, $p<0.05$, Student's t-test). Error bars represent ± SEM.

4.2.5 Dynamin inhibition causes loss of FM1-43 fluorescence independently of exocytosis

Having established that BoNT B completely blocks exocytosis (Figure 13), I was able to use this approach to control for the possibility that the decrease in fluorescence following dynamin inhibition was due to vesicle fusion and subsequent exocytosis. BoNT B was pressure injected into the axon as above (Figure 13), and control images were collected. Because I observed that the adjusted fluorescence levels reach a plateau following at least 1 hour of dynamin inhibition (Figure 10), fluorescence measurements of the relevant ROI were taken after an identical length of time of dynasore administration (Figure 14). As predicted, fluorescence decreased in FM1-43-loaded axons exposed to dynasore at rest, controlling for exocytosis with BoNT B ($n=5$, $p<0.005$, Student's t-test). To ensure exocytosis was still abolished via BoNT B, a second stimulation train was then applied (5Hz, 2000 stimuli) and images of the ROI were again collected. As expected, fluorescence did not decrease significantly below levels detected after 1 hour in either dynasore or control conditions ($n=5$, Student's t-test).

A

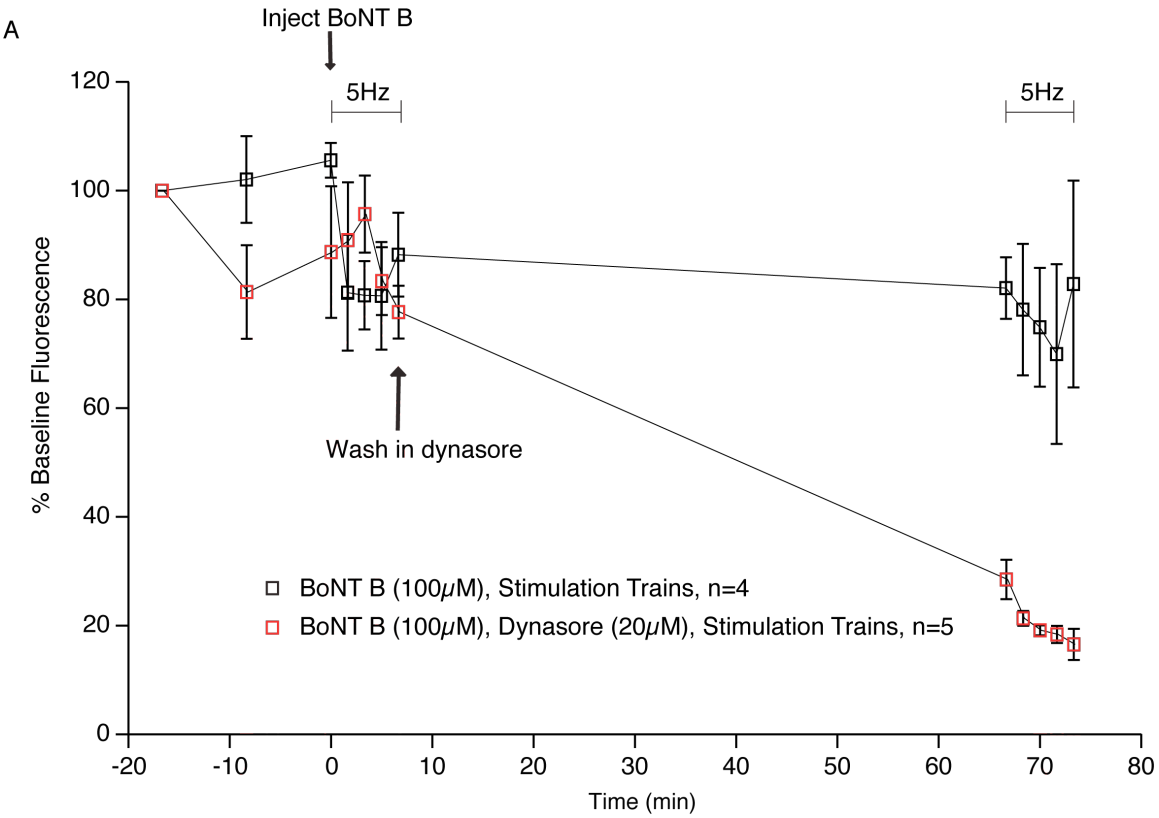
Inject BoNT B
5Hz
5Hz
Wash in dynasore
% Baseline Fluorescence
Time (min)
BoNT B (100μM), Stimulation Trains, n=4
BoNT B (100μM), Dynasore (20μM), Stimulation Trains, n=5
120
100
80
60
40
20
0
-20
-10
0
10
20
30
40
50
60
70
80

B

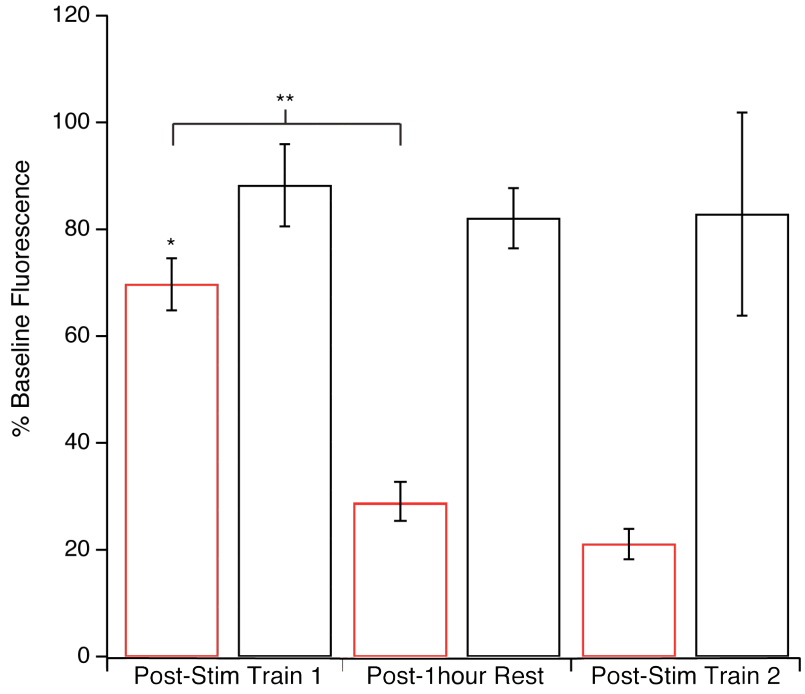
% Baseline Fluorescence
**
*
Post-Stim Train 1
Post-1hour Rest
Post-Stim Train 2
120
100
80
60
40
20
0

Figure 14. Dynasore (20μM) induces spontaneous loss of FM1-43 fluorescence when exocytosis is abolished by botulinum neurotoxin B light chain (BotNT B, 100μM). A. Following demonstration of stability of fluorescence at rest/baseline (n=13, black and red open squares), blockade of exocytosis was achieved as above via BotNT B microinjection. A stimulation train was applied to deplete the primed pool of vesicles (5Hz, 2000 stimuli), after which dynasore or control Ringer was washed onto the tissue for 1 hour. To demonstrate that exocytosis remained blocked, a second stimulation train (5Hz, 2000 stimuli) was applied. B. Bar graph comparing mean FM1-43 fluorescence values as a percent of baseline in tissue treated with BotNT B alone (black open squares, n=4) or with dynasore (red open squares, n=5). Following the first stimulation train (ST1) and a 1-hour rest period, tissue treated with BotNT B and dynasore exhibited a decrease to 18.1 ± 3.6% of baseline FM1-43 fluorescence (**, $p<0.005$, Student's t-test), after which no further depletion of fluorescence could be demonstrated via a second stimulation train (ST2). In contrast, tissue treated with BotNT B alone exhibited a decrease to 88.2 ± 7.7% of baseline FM1-43 fluorescence (NS, Student's t-test), after which the fluorescence remained stable after a 1-hour rest period and the second stimulation train (ST2). Error bars represent ± SEM.

4.2.6 Dynamin inhibition uncouples endocytosis and exocytosis.

Exocytosis and endocytosis are coupled processes in cells. This coupling ensures that cell membrane as well as vesicle pools are kept in balance. Endocytosis provides a means of (re-)entry into the cell, comprises half of the turnover machinery maintaining cell membrane surface area, and is necessary for vesicle formation. Loading of FM1-43 into presynaptic terminals can be achieved via stimulation dependent endocytosis in the presence of this styryl dye. Likewise, destaining of FM1-43-loaded vesicles can be achieved via stimulation which leads to fusion of vesicles with the cell membrane. In a large model synapse where the available vesicle pools are as sizeable as in the lamprey giant reticulospinal synapse, exocytosis will continue unabated during electrophysiological stimulation trains when endocytosis is inhibited.

As above, stimulation-dependent destaining (5Hz, 2000 stimuli) was observed by capturing and quantifying a *z*-stack of 3 images (images spaced 2μm apart) of the ROI every 500 stimuli. Fluorescence in FM1-43-loaded axons decreased to a mean of 41.2 ± 5.8% of baseline fluorescence (Figure 15). A cocktail of dynasore (20μM), DL-AP5 (100μM), and CNQX (10μM) was then washed onto destained axons for 10 minutes, after which FM1-43 was loaded via stimulation train as above (5Hz, 2000 stimuli). Consistent with previous studies showing that dynamin inhibition blocks endocytosis (Macia et al., 2006; Newton et al., 2006; Douthitt et al., 2011), dynasore (20μM) applied following destaining, but prior to a second loading of FM1-43, blocked CME. Specifically, FM1-43

fluorescence did not approach control values, but actually remained at or below the values determined following destaining.

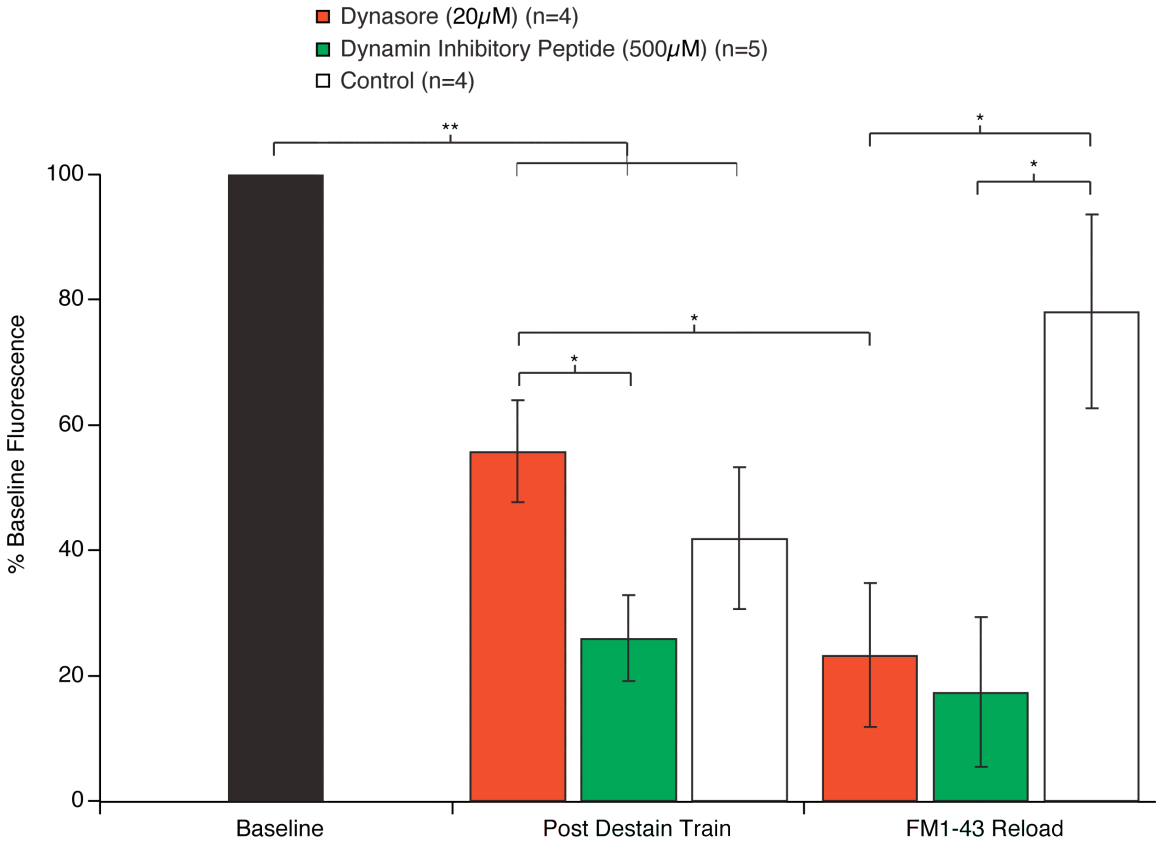
Dynasore (20μM) (n=4)
Dynamin Inhibitory Peptide (500μM) (n=5)
Control (n=4)
% Baseline Fluorescence
100
80
60
40
20
0
**
*
*
*
*
Baseline
Post Destain Train
FM1-43 Reload

Figure 15. Dynamin inhibition uncouples endocytosis from exocytosis. Following control FM1-43 loading (black), axons were destained via 5Hz stimulation (2000 stimuli). Upon reloading of FM1-43 (5Hz, 2000 stimuli), axons in which endocytosis was blocked with either dynasore or DIP exhibited no increase in fluorescence, whereas control axons did. (Error bars represent ± SEM; *, $p<0.05$; **, $p<0.005$, Student's t-test).

4.3 Discussion

A dynamin-1/2-like peptide is clearly responsible for vesicle scission during CME in the lamprey giant reticulospinal axon (Figure 15), but the evidence presented in this chapter indicates a further role for dynamin in maintaining vesicle pools in the resting presynaptic terminal (Figures 10-12, 14). It remains to be determined what proteins might be changing in response to acute dynamin inhibition in this large synapse. Other work showing potential upregulation of proteins responsible for phosphorylation of synapsins (Yao and Sakaba, 2012), modification of cytoskeletal proteins such as actin (Bähler and Greengard, 1987; Bloom, 2003; Ferguson et al., 2009; Taylor et al., 2012) has confirmed multiple proteins are responsible for maintaining vesicle pools even outside of those mediating endocytosis and exocytosis. Thus, future work will need to focus on changes in regulation of these proteins as a result of acute perturbation of dynamin, a protein now known as a potent regulator of resting vesicle pools, as well as one of the main known players in vesicle scission. Future ultrastructural studies examining dynamin inhibition using DIP, with/without the absence of exocytosis (via botulinum toxin b light chain, for instance) will also help to elucidate dynamin's role in the resting presynaptic terminal. In addition, longer time courses of dynamin inhibition may yield further reductions in vesicle pools, but this does not appear likely, as there appears to be a plateau of vesicle depletion based on FM1-43 fluorescence studies (Figure 10).

5. CONCLUDING REMARKS

5.1 A conserved player in clathrin-mediated endocytosis is not necessary for compensatory endocytosis during kiss-and run vesicle fusion

From our studies of FM1-43 destaining we know that tissue does not destain under conditions that shift the mode of vesicle fusion from full to kiss-and-run (Figure 6, also (Photowala et al., 2006)). Upon inhibition of a dynamin-1/2-like protein in the lamprey giant reticulospinal synapse, this resistance to destaining no longer persists, which fits well with my proposed mechanism, i.e., a retained fusion pore (Figure 7C) allowing more FM1-43 dye to continue to dissipate as it departitions from the lipid bilayer and still has access to the aqueous synaptic cleft. However, as Figure 8 illustrates, FM1-43 loading is still possible in the presence of 5-HT when dynamin is inhibited. It is still thus unclear why dynamin inhibition leads to such a paradoxical set of findings. Further experiments in which the dose of 5-HT, or the timing of dynamin inhibition relative to 5-HT-mediated presynaptic inhibition may further elucidate dynamin's role during this form of presynaptic plasticity.

This is the first piece of evidence documenting any possible conservation between vesicle retrieval during transient/kiss-and-run fusion and acquisition of nascent vesicles following completion of endocytosis (scission). It is not surprising that some proteins in such a highly conserved cellular function as clathrin-mediated endocytosis may function in other nuanced forms of vesicle regulation. It is energetically favorable for cells to conserve resources and diversify existing processes and proteins to a variety of functions. This is

arguably a hallmark of evolution.

5.2 Dynamin-1/2-like protein in a resting synapse

Thusfar, the role of the dynamin isoform present in a resting lamprey giant reticulospinal synapse remains a mystery. Inhibiting dynamin through two independent methods yielded unexpected results on FM1-43-loaded axons. Fluorescence of FM1-43-loaded axons decreased to a percentage of baseline fluorescence that was at or below the level present after a stimulus train applied to the axon (compare Figures 5, 10, and 14). However, evidence of dynamin's interactions with actin could be linked to our results. Dynamin controls its own recruitment to scission events via its modulation of the kinetics of actin and recruitment of other binding partners, e.g., N-BAR, to sites of scission; conversely, actin serves as a dynamic scaffold that concentrates dynamin and N-BAR proteins to these sites (Taylor et al., 2012). . Further work has revealed that dynamin plays a role in the actin polymerization-depolymerization cycle. Evidence has revealed interaction sites on residues of dynamin dimers and actin (Galletta et al., 2010; Mooren et al., 2012; Taylor et al., 2012), which is believed to mediate some of the interactions discussed above.

Regulation of a vesicle cycling, as discussed above, involves distinct proteins for both fusion and endocytosis, but pools of unprimed vesicles not actively fusing or forming are stored within cells until such time that they are competent for release. Synapsins, for instance, regulate synaptic vesicle clustering by facilitating tethering of vesicles to filamentous actin (F-actin)

(Giovedi, 2004; Messa et al., 2010). Cultured neurons from synapsin-1, -2, and -3 triple knockout (KO) mice display fewer synaptic vesicles at the active zone, but no difference in the number of primed vesicles (Stefani et al., 1997). Synapsin-1 appears to migrate close to an area within 100μm of the active zone during stimulation (Bloom, 2003), but it is argued that it is actually most likely associating with recently formed vesicles that are joining a pool of vesicles not yet primed for release, i.e., in the recycling pool. This makes sense because the F-actin tether mediated by synapsin is a hindrance to release, something which is regulated by calcium/calmodulin-dependent kinase II (CAM-KII) (Hosaka et al., 1999; Chi et al., 2003; Xia and Storm, 2005; Bykhovskaia, 2011). Phosphorylation of synapsin decreases its affinity for SVs and F-actin, which allows the vesicles to be targeted for fusion, as they are no longer bound to the cytoskeleton. Synapsins regulate vesicle storage and availability in a phosphorylation-dependent manner, which is tightly coupled to synaptic activity; for instance, synapsin-1 has been shown to bundle F-actin in a phosphorylation-dependent manner (Bähler and Greengard, 1987). Thus, activity in neuronal synapses requiring a high turnover of vesicles have higher rates of synapsin phosphorylation and dephosphorylation as vesicles are untethered from F-actin for release and re-tethered subsequent to completion of endocytosis, respectively (Bähler and Greengard, 1987). Interestingly, increased levels of phosph-βCAM-KII (threonine 286) have been found in primary neurons derived from dynamin-1/3 double knockout (DKO) mice (Lou et al., 2012), which raises the question of

whether acute dynamin inhibition causes a similar increase. Consistent with the notion of vesicles being tethered to F-actin in a phosphorylation-dependent manner, electron micrographs of synapses from these DKO mutants show a significant decrease in vesicles at the active zone. Thus, it is possible that the spontaneous decrease in FM1-43 fluorescence that I found in resting lamprey giant reticulospinal synapses exposed to dynasore or DIP (Figures 10 and 14) may be a result of degradation of a synapsin-1-like-dependent synaptic vesicle association with F-actin.

Furthermore, we clearly show that the effects of dynamin inhibition on FM1-43-loaded puncta at rest are not due to exocytosis because 1) FM1-43 fluorescence decreased following dynamin inhibition following blockade of exocytosis via microinjection of the light chain of botulinum neurotoxin b (Figure 14) and 2) no change in spontaneous release of glutamate was evident following dynasore administration (Figure 11). It is clear that a portion of the FM1-43-loaded pool of vesicles remains untouched via exocytosis or dynamin inhibition because a portion of baseline FM1-43 fluorescence remains in said axons (Figures 5, 10, 14). However, it is not clear whether these remaining pools differ. It is interesting to note that a stimulation train destains both primed and unprimed FM1-43-loaded vesicles, but dynamin inhibition via two separate techniques in axons at rest yielded similar decreases in FM1-43 fluorescence.

From electrophysiological recordings of post-synaptic cells in the lamprey spinal cord (neurons onto which reticulospinal neurons synapse), mEPSC

amplitude and frequency were unaffected by dynasore (Figure 11). However, spontaneous uptake of either of two different styryl dyes (FM1-43 and FM2-10, a styryl dye less hydrophobic than FM1-43) was decreased upon exposure to dynasore (Chung et al., 2010). However this latter finding was done using a 4-fold-higher concentration of dynasore (80μM) in mouse primary cortical neurons which have considerably smaller vesicle pools than those present in the lamprey giant reticulospinal synapse. Thus, the impact of a higher concentration of dynasore, coupled with a smaller relative SV pool size could explain why it was not seen in my preparation.

Dynamin inhibition clearly uncouples endocytosis and exocytosis because FM1-43 loading is blocked relative to loading and/or reloading in control lamprey Ringer (Figure 15). Because a short window (10 min) is allowed for either dynasore or DIP to exert their respective effects prior to the stimulus train for re-loading FM1-43, it is possible that some of the remaining fluorescence after destaining is lost due to an interaction of dynamin with resting vesicles that we have just begun to reveal through well controlled experiments inhibiting dynamin-1/2-like isoform in the lamprey. It is thus unclear whether a proportion of the FM1-43-loaded vesicles remaining after control loading and destaining is affected by dynamin inhibition at rest. It is possible that these two modes of decreasing FM1-43 fluorescence act on different vesicle pools. Further experiments in which FM1-43 loaded axons are destained via stimulation to a plateau and then exposed to dynamin inhibition (or the reverse order) could be used to answer this

question. If the pools are separate, I would predict that FM1-43 fluorescence would continue to decrease regardless of whether tissue was stimulated or exposed to dynamin inhibitors at rest.

CITED LITERATURE

Adler EM, **Augustine GJ**, **Duffy SN**, **Charlton MP**. Alien intracellular calcium chelators attenuate neurotransmitter release at the squid giant synapse. *Journal of Neuroscience* 11: 1496–1507, 1991.

Alford S, **Grillner S**. CNQX and DNQX block non-NMDA synaptic transmission but not NMDA-evoked locomotion in lamprey spinal cord. *Brain Res* 506: 297–302, 1990.

Anggono V, **Robinson PJ**. Syndapin I and endophilin I bind overlapping proline-rich regions of dynamin I: role in synaptic vesicle endocytosis. *J Neurosci Methods* 102: 931–943, 2007.

Anggono V, **Smillie KJ**, **Graham ME**, **Valova VA**, **Cousin MA**, **Robinson PJ**. Syndapin I is the phosphorylation-regulated dynamin I partner in synaptic vesicle endocytosis. *Nat Neurosci* 9: 752–760, 2006.

Aravanis AM, **Pyle JL**, **Harata NC**, **Tsien RW**. Imaging single synaptic vesicles undergoing repeated fusion events: kissing, running, and kissing again. *Neuropharmacology* 45: 797–813, 2003a.

Aravanis AM, **Pyle JL**, **Tsien RW**. Single synaptic vesicles fusing transiently and successively without loss of identity. *Nature* 423: 643–647, 2003b.

Archer DA, **Graham ME**, **Burgoyne RD**. Complexin regulates the closure of the fusion pore during regulated vesicle exocytosis. *J Biol Chem* 277: 18249–18252, 2002.

Artalejo CR, **Elhamdani A**, **Palfrey HC**. Secretion: dense-core vesicles can kiss-and-run too. *Curr Biol* 8: R62–5, 1998a.

Artalejo CR, **Elhamdani A**, **Palfrey HC**. Secretion: Dense-core vesicles can kiss-and-run too. *Curr Biol* 8: 0–0, 1998b.

Asztely F, **Erdemli G**, **Kullmann DM**. Extrasynaptic Glutamate Spillover in the Hippocampus: Dependence on Temperature and the Role of Active Glutamate Uptake. *Neuron* 18: 13–13, 1997.

Bai J, **Wang C-T**, **Richards DA**, **Jackson MB**, **Chapman ER**. Fusion Pore Dynamics Are Regulated by Synaptotagmin*t-SNARE Interactions. *Neuron* 41: 14–14, 2004.

Barbeau H, **Rossignol S**. The effects of serotonergic drugs on the locomotor pattern and on cutaneous reflexes of the adult chronic spinal cat. *Brain Res* 514: 55–67, 1990.

Barreiro-Iglesias A, **Villar-Cerviño V**, **Anadón R**, **Rodicio MC**. Development and organization of the descending serotonergic brainstem–spinal projections in the sea lamprey. *Journal of Chemical Neuroanatomy* 36: 77–84, 2008.

Bähler M, **Greengard P**. Synapsin I bundles F-actin in a phosphorylation-dependent manner. *Nature* 326: 704–707, 1987.

Betz WJ, **Bewick GS**, **Ridge RM**. Intracellular movements of fluorescently labeled synaptic vesicles in frog motor nerve terminals during nerve stimulation. *Neuron* 9: 805–813, 1992a.

Betz WJ, **Bewick GS**. Optical monitoring of transmitter release and synaptic vesicle recycling at the frog neuromuscular junction. *The Journal of Physiology* 460: 287–309, 1993.

Betz WJ, **Mao F**, **Bewick GS**. Activity-dependent fluorescent staining and destaining of living vertebrate motor nerve terminals. *Journal of Neuroscience* 12: 363–375, 1992b.

Betz WJ, **Ridge RM**, **Bewick GS**. Comparison of FM1-43 staining patterns and electrophysiological measures of transmitter release at the frog neuromuscular junction. *J Physiol Paris* 87: 193–202, 1993.

Blackmer T, **Larsen EC**, **Bartleson C**, **Kowalchyk JA**, **Yoon E-J**, **Preininger AM**, **Alford S**, **Hamm HE**, **Martin TFJ**. G protein betagamma directly regulates SNARE protein fusion machinery for secretory granule exocytosis. *Nature Publishing Group* 8: 421–425, 2005.

Blackmer T, **Larsen EC**, **Takahashi M**, **Martin TF**, **Alford S**, **Hamm HE**. G protein betagamma subunit-mediated presynaptic inhibition: regulation of exocytotic fusion downstream of Ca2+ entry. *Science* 292: 293–297, 2001.

Blanton MG, **Turco Lo JJ**, **Kriegstein AR**. Whole cell recording from neurons in slices of reptilian and mammalian cerebral cortex. *J Neurosci Methods* 30: 203–210, 1989.

Bleckert A, **Photowala H**, **Alford S**. Dual pools of actin at presynaptic terminals. *Journal of Neurophysiology* 107: 3479–3492, 2012.

Bloom O. Colocalization of synapsin and actin during synaptic vesicle recycling. *The Journal of Cell Biology* 161: 737–747, 2003.

Boucrot E, **Pick A**, **Çamdere G**, **Liska N**, **Evergren E**, **McMahon HT**, **Kozlov MM**. Membrane Fission Is Promoted by Insertion of Amphipathic Helices and Is Restricted by Crescent BAR Domains. *Cell* 149: 124–136, 2012.

Broadie KK, **Prokop AA**, **Bellen HJH**, **O'Kane CJC**, **Schulze KLK**, **Sweeney STS**. Syntaxin and synaptobrevin function downstream of vesicle docking in Drosophila. *Neuron* 15: 663–673, 1995.

Brodin L, **Shupliakov O**, **Pieribone VA**, **Hellgren J**, **Hill RH**. The reticulospinal glutamate synapse in lamprey: plasticity and presynaptic variability. *Journal of Neurophysiology* 72: 592–604, 1994.

Buchanan JTJ, **Grillner SS**. 5-Hydroxytryptamine depresses reticulospinal excitatory postsynaptic potentials in motoneurons of the lamprey. *Neurosci Lett* 122: 71–44, 1991.

Büschges A, **Scholz H**, **Manira El A**. New Moves in Motor Control. *Curr Biol* 21: R513–R524, 2011.

Bykhovskaia M. Synapsin regulation of vesicle organization and functional pools. *Seminars in Cell and Developmental Biology* 22: 387–392, 2011.

Ceccarelli B, **Hurlbut WP**, **Mauro A**. Turnover of transmitter and synaptic vesicles at the frog neuromuscular junction. *The Journal of Cell Biology* 57: 499–524, 1973.

Chen GG, **Harata NCN**, **Tsien RWR**. Paired-pulse depression of unitary quantal amplitude at single hippocampal synapses. *Proc Natl Acad Sci USA* 101: 1063–1068, 2004a.

Chen S, **Barbieri JT**. Association of botulinum neurotoxin serotype A light chain with plasma membrane-bound SNAP-25. *J Biol Chem* 286: 15067–15072, 2011.

Chen X, **Tang J**, **Sudhof TC**, **Rizo J**. Are neuronal SNARE proteins Ca2+ sensors? *Journal of molecular biology* 347: 145–158, 2005a.

Chen X, **Wang L**, **Zhou Y**, **Zheng LH**, **Zhou Z**. “Kiss-and-run” glutamate secretion in cultured and freshly isolated rat hippocampal astrocytes. *J Neurosci* 25: 9236–9243, 2005b.

Chen X-K, **Wang L-C**, **Zhou Y**, **Cai Q**, **Prakriya M**, **Duan K-L**, **Sheng Z-H**, **Lingle C**, **Zhou Z**. Activation of GPCRs modulates quantal size in chromaffin cells through Gβγ and PKC. *Nat Neurosci* 8: 1160–1168, 2005c.

Chen Y-J, **Zhang P**, **Egelman EH**, **Hinshaw JE**. The stalk region of dynamin drives the constriction of dynamin tubes. *Nat Struct Mol Biol* v11: 574–575, 2004b.

Chi P, **Greengard P**, **Ryan TA**. Synaptic vesicle mobilization is regulated by distinct synapsin I phosphorylation pathways at different frequencies. *Neuron* 38:

69–78, 2003.

Choi S, **Klingauf J**, **Tsien RW**. Postfusional regulation of cleft glutamate concentration during LTP at“silent synapses.” *Nat Neurosci* 3: 330–336, 2000.

Choi S, **Klingauf J**, **Tsien RW**. Fusion pore modulation as a presynaptic mechanism contributing to expression of long-term potentiation. *Philosophical Transactions of the Royal Society B: Biological Sciences* 358: 695–705, 2003.

Chung C, **Barylko B**, **Leitz J**, **Liu X**, **Kavalali ET**. Acute Dynamin Inhibition Dissects Synaptic Vesicle Recycling Pathways That Drive Spontaneous and Evoked Neurotransmission. *J Neurosci* 30: 1363–1376, 2010.

Chung C, **Kavalali ET**. Synaptic Vesicle Endocytosis: Get Two for the Price of One? *Neuron* 61: 333–334, 2009.

Cochilla AJ, **Alford S**. Glutamate receptor-mediated synaptic excitation in axons of the lamprey. *The Journal of Physiology* 499 (Pt 2): 443–457, 1997.

Cochilla AJ, **Angleson JK**, **Betz WJ**. Monitoring secretory membrane with FM1-43 fluorescence. *Annu Rev Neurosci* 22: 1–10, 1999.

Cousin MA, **Robinson PJ**. Mechanisms of synaptic vesicle recycling illuminated by fluorescent dyes. *J Neurosci Methods* 73: 2227–2239, 1999.

Davies J, **Watkins JC**. Actions of D and L forms of 2-amino-5-phosphonovalerate and 2-amino-4-phosphonobutyrate in the cat spinal cord. *Brain Res* 235: 378–386, 1982.

Deak F, **Schoch S**, **Liu X**, **Sudhof TC**, **Kavalali ET**. Synaptobrevin is essential for fast synaptic-vesicle endocytosis. *Nature cell biology* 6: 1102–1108, 2004.

Deitcher DLD, **Ueda AA**, **Stewart BAB**, **Burgess RWR**, **Kidokoro YY**, **Schwarz TLT**. Distinct requirements for evoked and spontaneous release of neurotransmitter are revealed by mutations in the Drosophila gene neuronal-synaptobrevin. *Journal of Neuroscience* 18: 2028–2039, 1998.

del Castillo J, **Katz B**. Quantal components of the end-plate potential [Online]. *The Journal of Physiology* 124: 560–573, 1954. http://courses.northwestern.edu/@@815FC2EC0A63D6D345995DE9D12908B6/courses/1/2009WI_NUIN_411-2_SEC01/content/_1591646_1/Del%20Castillo%20and%20Katz%201954a.pdf.

Delgado R, **Maureira C**, **Oliva C**, **Kidokoro Y**, **Labarca P**. Size of vesicle pools, rates of mobilization, and recycling at neuromuscular synapses of a Drosophila mutant, shibire. *Neuron* 28: 941–953, 2000.

Dickman DK, **Horne JA**, **Meinertzhagen IA**, **Schwarz TL**. A slowed classical pathway rather than kiss-and-run mediates endocytosis at synapses lacking synaptojanin and endophilin. *Cell* 123: 521–533, 2005.

Dittman J, **Ryan TA**. Molecular Circuitry of Endocytosis at Nerve Terminals. *Annu. Rev. Cell Dev. Biol.* 25: 133–160, 2009.

Douthitt HL, **Luo F**, **McCann SD**, **Meriney SD**. Dynasore, an inhibitor of dynamin, increases the probability of transmitter release. *Neuroscience* 172: 187–195, 2011.

Doxsey SJ, **Brodsky FM**, **Blank GS**, **Helenius A**. Inhibition of endocytosis by anti-clathrin antibodies. *Cell* 50: 453–463, 1987.

Elhamdani A, **Palfrey HC**, **Artalejo CR**. Quantal size is dependent on stimulation frequency and calcium entry in calf chromaffin cells. *Neuron* 31: 819–830, 2001.

Evergren E, **Zotova E**, **Brodin L**, **Shupliakov O**. Differential efficiency of the endocytic machinery in tonic and phasic synapses. *Neuroscience* 141: 123–131, 2006.

Faelber K, **Held M**, **Gao S**, **Posor Y**, **Haucke V**, **Noé F**, **Daumke O**. Structural Insights into Dynamin-Mediated Membrane Fission. *Structure/Folding and Design* 20: 1621–1628, 2012.

Fatt P, **Katz B**. Spontaneous subthreshold activity at motor nerve endings. *The Journal of Physiology* 117: 109–128, 1952.

Ferguson S, **Raimondi A**, **Paradise S**, **Shen H**, **Mesaki K**, **Ferguson A**, **Destaing O**, **Ko G**, **Takasaki J**, **Cremona O**, **Toole EO**, **Pietro De Camilli**. Coordinated Actions of Actin and BAR Proteins Upstream of Dynamin at Endocytic Clathrin-Coated Pits. *Dev Cell* 17: 811–822, 2009.

Ford MGJM, **Mills IGI**, **Peter BJB**, **Vallis YY**, **Praefcke GJKG**, **Evans PRP**, **McMahon HTH**. Curvature of clathrin-coated pits driven by epsin. *Nature* 419: 361–366, 2002.

Gaffield MA, **Rizzoli SO**, **Betz WJ**. Mobility of synaptic vesicles in different pools in resting and stimulated frog motor nerve terminals. *Neuron* 51: 317–325, 2006.

Galletta BJ, **Cooper JA**. Actin and endocytosis: mechanisms and phylogeny. *Current opinion in cell biology* 21: 20–27, 2009.

Galletta BJ, **Mooren OL**, **Cooper JA**. Actin dynamics and endocytosis in yeast and mammals. *Current Opinion in Biotechnology* 21: 604–610, 2010.

Gandhi SPS, **Stevens CFC**. Three modes of synaptic vesicular recycling revealed by single-vesicle imaging. *Nature* 423: 607–613, 2003.

Gerachshenko T, **Blackmer T**, **Yoon EJ**, **Bartleson C**, **Hamm HE**, **Alford S**. Gbetagamma acts at the C terminus of SNAP-25 to mediate presynaptic inhibition. *Nature Publishing Group* 8: 597–605, 2005.

Gerachshenko T, **Schwartz E**, **Bleckert A**, **Photowala H**, **Seymour A**, **Alford S**. Presynaptic G-Protein-Coupled Receptors Dynamically Modify Vesicle Fusion, Synaptic Cleft Glutamate Concentrations, and Motor Behavior. *J Neurosci* 29: 10221–10233, 2009a.

Gerachshenko T, **Schwartz E**, **Bleckert A**, **Photowala H**, **Seymour A**, **Alford S**. Presynaptic G-Protein-Coupled Receptors Dynamically Modify Vesicle Fusion, Synaptic Cleft Glutamate Concentrations, and Motor Behavior. *J Neurosci* 29: 10221–10233, 2009b.

Giovedi S. Synapsin Is a Novel Rab3 Effector Protein on Small Synaptic Vesicles: II. FUNCTIONAL EFFECTS OF THE Rab3A-SYNAPSIN I INTERACTION. *Journal of Biological Chemistry* 279: 43769–43779, 2004.

Gitler D, **Cheng Q**, **Greengard P**, **Augustine GJ**. Synapsin IIa Controls the Reserve Pool of Glutamatergic Synaptic Vesicles. *J Neurosci* 28: 10835–10843, 2008.

Glyvuk N, **Tsytsyura Y**, **Geumann C**, **Hooge RDA**, **ve JHU**, **Kratzke M**, **Baltes J**, **ning DBO**, **Klingauf JUR**, **Schu P**. AP-1/σ1B-adaptin mediates endosomal synaptic vesicle recycling, learning and memory. *The EMBO Journal* (March 4, 2010). doi: 10.1038/emboj.2010.15.

Graham ME, **Fisher RJ**, **Burgoyne RD**. Measurement of exocytosis by amperometry in adrenal chromaffin cells: effects of clostridial neurotoxins and activation of protein kinase C on fusion pore kinetics. *Biochimie* 82: 469–479, 2000.

Granseth B, **Odermatt B**, **Royle SJ**, **Lagnado L**. Clathrin-mediated endocytosis is the dominant mechanism of vesicle retrieval at hippocampal synapses. *Neuron* 51: 773–786, 2006.

Groemer TW, **Klingauf J**. Synaptic vesicles recycling spontaneously and during activity belong to the same vesicle pool. *Nature Publishing Group* 10: 145–147, 2007.

Gustafsson JS, **Birinyi AS**, **Crum J**, **Ellisman M**, **Brodin L**, **Shupliakov O**. Ultrastructural organization of lamprey reticulospinal synapses in three dimensions. *J Comp Neurol* 450: 167–182, 2002.

Gutierrez LM. New insights into the role of the cortical cytoskeleton in exocytosis from neuroendocrine cells. *Int Rev Cell Mol Biol* 295: 109–137, 2012.

Hammarlund M, **Palfreyman MT**, **Watanabe S**, **Olsen S**, **Jorgensen EM**. Open syntaxin docks synaptic vesicles. *PLoS Biol* 5: e198, 2007.

Harata NC, **Aravanis AM**, **Tsien RW**. Kiss-and-run and full-collapse fusion as modes of exo-endocytosis in neurosecretion. *J Neurosci Methods* 97: 1546–1570, 2006a.

Harata NC, **Choi S**, **Pyle JL**, **Aravanis AM**, **Tsien RW**. Frequency-dependent kinetics and prevalence of kiss-and-run and reuse at hippocampal synapses studied with novel quenching methods. *Neuron* 49: 243–256, 2006b.

Hartig SM, **Ishikura S**, **Hicklen RS**, **Feng Y**, **Blanchard EG**, **Voelker KA**, **Pichot CS**, **Grange RW**, **Raphael RM**, **Klip A**, **Corey SJ**. The F-BAR protein CIP4 promotes GLUT4 endocytosis through bidirectional interactions with N-WASp and Dynamin-2. *J. Cell. Sci.* 122: 2283–2291, 2009.

Harvey VL, **Stephens GJ**. Mechanism of GABAB receptor-mediated inhibition of spontaneous GABA release onto cerebellar Purkinje cells. *Eur J Neurosci* 20: 684–700, 2004.

Hayashi TT, **McMahon HH**, **Yamasaki SS**, **Binz TT**, **Hata YY**, **Südhof TCT**, **Niemann HH**. Synaptic vesicle membrane fusion complex: action of clostridial neurotoxins on assembly. *EMBO J* 13: 5051–5061, 1994.

He L, **Wu LG**. The debate on the kiss-and-run fusion at synapses. *Trends Neurosci* 30: 447–455, 2007.

He L, **Wu X-S**, **Mohan R**, **Wu L-G**. Two modes of fusion pore opening revealed by cell-attached recordings at a synapse. *Nature* 444: 102–105, 2006.

Henkel AW, **Lubke J**, **Betz WJ**. FM1-43 dye ultrastructural localization in and release from frog motor nerve terminals. *Proc Natl Acad Sci USA* 93: 1918–1923, 1996.

Henmi Y, **Tanabe K**, **Takei K**. Disruption of Microtubule Network Rescues Aberrant Actin Comets in Dynamin2-Depleted Cells. *PLoS ONE* 6: e28603, 2011.

Heuser JE, **Reese TS**, **Dennis MJ**, **Jan Y**, **Jan L**, **Evans L**. Synaptic vesicle exocytosis captured by quick freezing and correlated with quantal transmitter release. *The Journal of Cell Biology* 81: 275–300, 1979.

Hinshaw JE, **Schmid SL**. Dynamin self-assembles into rings suggesting a mechanism for coated vesicle budding. *Nature* 374: 190–192, 1995.

Hosaka M, **Hammer RE**, **Sudhof TC**. A phospho-switch controls the dynamic association of synapsins with synaptic vesicles. *Neuron* 24: 377–387, 1999.

Jarousse N, **Kelly RB**. Endocytotic mechanisms in synapses. *Current opinion in cell biology* 13: 461–469, 2001.

Jörntell H, **Hansel C**. Synaptic memories upside down: bidirectional plasticity at cerebellar parallel fiber-Purkinje cell synapses. *Neuron* 52: 227–238, 2006.

Jung N, **Haucke V**. Clathrin-Mediated Endocytosis at Synapses. *Traffic (Copenhagen, Denmark)* 8: 1129–1136, 2007.

Kao CY. Pharmacology of tetrodotoxin and saxitoxin. [Fed Proc. 1972 May-Jun] - PubMed - NCBI. *Fed Proc* 31: 1117–1123, 1972.

Kavalali ET, **Klingauf J**, **Tsien RW**. Properties of fast endocytosis at hippocampal synapses. *Philosophical Transactions of the Royal Society B: Biological Sciences* 354: 337–346, 1999.

Kay AR, **Alfonso A**, **Alford S**, **Cline HT**, **Holgado AM**, **Sakmann B**, **Snitsarev VA**, **Stricker TP**, **Takahashi M**, **Wu LG**. Imaging synaptic activity in intact brain and slices with FM1-43 in C. elegans, lamprey, and rat. *Neuron* 24: 809–817, 1999.

Kessels MM. The syndapin protein family: linking membrane trafficking with the cytoskeleton. *J. Cell. Sci.* 117: 3077–3086, 2004.

Kessels MM. Syndapin Oligomers Interconnect the Machineries for Endocytic Vesicle Formation and Actin Polymerization. *J Biol Chem* 281: 13285–13299, 2006.

Kirchhausen T, **Macia E**, **Pelish HE**. Use of dynasore, the small molecule inhibitor of dynamin, in the regulation of endocytosis. *Methods in enzymology* 438: 77–93, 2008.

Klyachko VA, **Jackson MB**. Capacitance steps and fusion pores of small and large-dense-core vesicles in nerve terminals. *Nature* 418: 89–92, 2002.

Koticha DK, **McCarthy EE**, **Baldini G**. Plasma membrane targeting of SNAP-25 increases its local concentration and is necessary for SNARE complex formation and regulated exocytosis. *J. Cell. Sci.* 115: 3341–3351, 2002.

Körber C, **Horstmann H**, **Sätzler K**, **Kuner T**. Endocytic Structures and Synaptic Vesicle Recycling at a Central Synapse in Awake Rats. *Traffic (Copenhagen, Denmark)* (October 3, 2012). doi: 10.1111/tra.12007.

Kuromi H, **Kidokoro Y**. Two distinct pools of synaptic vesicles in single

presynaptic boutons in a temperature-sensitive Drosophila mutant, shibire. *Neuron* 20: 917–925, 1998.

Lam BC-H, **Sage TL**, **Bianchi F**, **Blumwald E**. Regulation of ADL6 activity by its associated molecular network. *Plant J.* 31: 565–576, 2002.

Lee S, **Jung K-Y**, **Park J**, **Cho J-H**, **Kim Y-C**, **Chang S**. Synthesis of potent chemical inhibitors of dynamin GTPase. *Bioorg Med Chem Lett* 20: 4858–4864, 2010.

Liao D, **Hessler NA**, **Malinow R**. Activation of postsynaptically silent synapses during pairing-induced LTP in CA1 region of hippocampal slice. *Nature* 375: 400–404, 2002.

Littleton JTJ, **Chapman ERE**, **Kreber RR**, **Garment MBM**, **Carlson SDS**, **Ganetzky BB**. Temperature-Sensitive Paralytic Mutations Demonstrate that Synaptic Exocytosis Requires SNARE Complex Assembly and Disassembly. *Neuron* 21: 13–13, 1998.

Lou X, **Fan F**, **Messa M**, **Raimondi A**, **Wu Y**, **Looger LL**, **Ferguson SM**, **De Camilli P**. Reduced release probability prevents vesicle depletion and transmission failure at dynamin mutant synapses. *Proceedings of the National Academy of Sciences* 109: E515–23, 2012.

Lu W, **Ma H**, **Sheng Z-H**, **Mochida S**. Dynamin and activity regulate synaptic vesicle recycling in sympathetic neurons. *J Biol Chem* 284: 1930–1937, 2009.

Macia E, **Ehrlich M**, **Massol R**, **Boucrot E**, **Brunner C**, **Kirchhausen T**. Dynasore, a cell-permeable inhibitor of dynamin. *Dev Cell* 10: 839–850, 2006.

Mears JA, **Ray P**, **Hinshaw JE**. A Corkscrew Model for Dynamin Constriction. *Structure* 15: 1190–1202, 2007.

Mehta PP, **Battenberg E**, **Wilson MC**. SNAP-25 and synaptotagmin involvement in the final Ca(2+)-dependent triggering of neurotransmitter exocytosis. *Proc Natl Acad Sci USA* 93: 10471–10476, 1996.

Merrifield CJ, **Perrais D**, **Zenisek D**. Coupling between Clathrin-Coated-Pit Invagination, Cortactin Recruitment, and Membrane Scission Observed in Live Cells. *Cell* 121: 593–606, 2005.

Messa M, **Congia S**, **Defranchi E**, **Valtorta F**, **Fassio A**, **Onofri F**, **Benfenati F**. Tyrosine phosphorylation of synapsin I by Src regulates synaptic-vesicle trafficking. *J. Cell. Sci.* 123: 2256–2265, 2010.

Mettlen M, **Pucadyil T**, **Ramachandran R**, **Schmid SL**. Dissecting dynamin's

role in clathrin-mediated endocytosis. *Biochem. Soc. Trans* 37: 1022, 2009.

Mooren OL, **Galletta BJ**, **Cooper JA**. Roles for Actin Assembly in Endocytosis. *Annu. Rev. Biochem.* 81: 661–686, 2012.

Morgan JR, **Augustine GJ**, **Lafer EM**. Synaptic vesicle endocytosis: the races, places, and molecular faces. *Neuromolecular medicine* 2: 101–114, 2002.

Nankoe SR, **Sever S**. Dynasore puts a new spin on dynamin: a surprising dual role during vesicle formation. *Trends in cell biology* 16: 607–609, 2006.

Neale EA, **Bowers LM**, **Jia M**, **Bateman KE**, **Williamson LC**. Botulinum neurotoxin A blocks synaptic vesicle exocytosis but not endocytosis at the nerve terminal. *The Journal of Cell Biology* 147: 1249–1260, 1999.

Newton AJ, **Kirchhausen T**, **Murthy VN**. Inhibition of dynamin completely blocks compensatory synaptic vesicle endocytosis. *Proc Natl Acad Sci USA* 103: 17955–17960, 2006.

Nurrish S, **Ségalat L**, **Kaplan JM**. Serotonin inhibition of synaptic transmission: Gαo decreases the abundance of UNC-13 at release sites. *Neuron* 24: 231–242, 1999.

Palfrey HC, **Artalejo CR**. Secretion: kiss and run caught on film. *Curr Biol* 13: R397–9, 2003.

Pawlu CC, **DiAntonio AA**, **Heckmann MM**. Postfusional Control of Quantal Current Shape. *Neuron* 42: 12–12, 2004.

Photowala H, **Blackmer T**, **Schwartz E**, **Hamm HE**, **Alford S**. G protein betagamma-subunits activated by serotonin mediate presynaptic inhibition by regulating vesicle fusion properties. *Proc Natl Acad Sci USA* 103: 4281–4286, 2006.

Photowala H, **Freed R**, **Alford S**. Location and function of vesicle clusters, active zones and Ca2+ channels in the lamprey presynaptic terminal. *The Journal of Physiology* 569: 119–135, 2005.

Pieribone VA, **Shupliakov O**, **Brodin L**, **Hilfiker-Rothenfluh S**, **Czernik AJ**, **Greengard P**. Distinct pools of synaptic vesicles in neurotransmitter release. *Nature* 375: 493–497, 1995.

Praefcke GJK, **McMahon HT**. The dynamin superfamily: universal membrane tubulation and fission molecules? *Nat Rev Mol Cell Biol* 5: 133–147, 2004.

Pucadyil TJ, **Schmid SL**. Conserved Functions of Membrane Active GTPases in Coated Vesicle Formation. *Science* 325: 1217–1220, 2009.

Pyle JLJ, **Kavalali ETE**, **Piedras-Rentería ESE**, **Tsien RWR**. Rapid Reuse of Readily Releasable Pool Vesicles at Hippocampal Synapses. *Neuron* 28: 11–11, 2000.

Richards DA. Two modes of exocytosis at hippocampal synapses revealed by rate of FM1-43 efflux from individual vesicles. *The Journal of Cell Biology* 168: 929–939, 2005.

Rickman C, **Archer DA**, **Meunier FA**, **Craxton M**, **Fukuda M**, **Burgoyne RD**, **Davletov B**. Synaptotagmin interaction with the syntaxin/SNAP-25 dimer is mediated by an evolutionarily conserved motif and is sensitive to inositol hexakisphosphate. *J Biol Chem* 279: 12574–12579, 2004.

Ringstad N, **Nemoto Y**, **De Camilli P**. Differential expression of endophilin 1 and 2 dimers at central nervous system synapses. *J Biol Chem* 276: 40424–40430, 2001.

Rizzoli SO, **Jahn R**. Kiss-and-run, collapse and “readily retrievable” vesicles. *Traffic (Copenhagen, Denmark)* 8: 1137–1144, 2007.

Rossi DJ, **Alford S**, **Mugnaini E**, **Slater NT**. Properties of transmission at a giant glutamatergic synapse in cerebellum: the mossy fiber-unipolar brush cell synapse. *Journal of Neurophysiology* 74: 24–42, 1995.

Roux A, **Uyhazi K**, **Frost A**, **De Camilli P**. GTP-dependent twisting of dynamin implicates constriction and tension in membrane fission. *Nature* 441: 528–531, 2006.

Sakaba T, **Neher E**. Direct modulation of synaptic vesicle priming by GABA(B) receptor activation at a glutamatergic synapse. *Nature* 424: 775–778, 2003.

Schiavo G, **Benfenati F**, **Poulain B**, **Rossetto O**, **Polverino de Laureto P**, **DasGupta BR**, **Montecucco C**. Tetanus and botulinum-B neurotoxins block neurotransmitter release by proteolytic cleavage of synaptobrevin. *Nature* 359: 832–835, 1992.

Schiavo G, **Stenbeck G**, **Rothman JE**, **Sollner TH**. Binding of the synaptic vesicle v-SNARE, synaptotagmin, to the plasma membrane t-SNARE, SNAP-25, can explain docked vesicles at neurotoxin-treated synapses. *Proc Natl Acad Sci USA* 94: 997–1001, 1997.

Schmid SL, **Frolov VA**. Dynamin: Functional Design of a Membrane Fission Catalyst. *Annu. Rev. Cell Dev. Biol.* 27: 79–105, 2011.

Schneider SW. Kiss and run mechanism in exocytosis. *The Journal of membrane biology* 181: 67–76, 2001.

Schwartz EJ, **Blackmer T**, **Gerachshenko T**, **Alford S**. Presynaptic G-protein-coupled receptors regulate synaptic cleft glutamate via transient vesicle fusion. *J Neurosci* 27: 5857–5868, 2007.

Schwartz EJ, **Gerachshenko T**, **Alford S**. 5-HT prolongs ventral root bursting via presynaptic inhibition of synaptic activity during fictive locomotion in lamprey. *Journal of Neurophysiology* 93: 980–988, 2004.

Shupliakov O, **Brodin L**. Recent insights into the building and cycling of synaptic vesicles. *Experimental Cell Research* 316: 1344–1350, 2010.

Shupliakov O, **Low P**, **Grabs D**, **Gad H**, **Chen H**, **David C**, **Takei K**, **De Camilli P**, **Brodin L**. Synaptic vesicle endocytosis impaired by disruption of dynamin-SH3 domain interactions. *Science* 276: 259–263, 1997.

Silinsky EM. On the mechanism by which adenosine receptor activation inhibits the release of acetylcholine from motor nerve endings. *The Journal of Physiology* 346: 243–256, 1984.

Sillar KT, **Simmers AJ**. 5HT induces NMDA receptor-mediated intrinsic oscillations in embryonic amphibian spinal neurons. *Proc. Biol. Sci.* 255: 139–145, 1994.

Sillar KT, **Wedderburn JF**, **Simmers AJ**. Modulation of swimming rhythmicity by 5-hydroxytryptamine during post-embryonic development in Xenopus laevis. *Proc. Biol. Sci.* 250: 107–114, 1992.

Smillie KJ, **Cousin MA**. Dynamin I phosphorylation and the control of synaptic vesicle endocytosis. *Biochem. Soc. Symp.* : 87–97, 2005.

Stanton PK, **Winterer J**, **Zhang XL**, **Muller W**. Imaging LTP of presynaptic release of FM1-43 from the rapidly recycling vesicle pool of Schaffer collateral-CA1 synapses in rat hippocampal slices. *Eur J Neurosci* 22: 2451–2461, 2005.

Stefani G, **Onofri F**, **Valtorta F**, **Vaccaro P**, **Greengard P**, **Benfenati F**. Kinetic analysis of the phosphorylation-dependent interactions of synapsin I with rat brain synaptic vesicles. *The Journal of Physiology* 504 (Pt 3): 501–515, 1997.

Stowell MH, **Marks B**, **Wigge P**, **McMahon HT**. Nucleotide-dependent conformational changes in dynamin: evidence for a mechanochemical molecular spring. *Nature cell biology* 1: 27–32, 1999.

Sudhof TC. The synaptic vesicle cycle revisited. *Neuron* 28: 317–320, 2000.

Sundborger A, **Soderblom C**, **Vorontsova O**, **Evergren E**, **Hinshaw JE**, **Shupliakov O**. An endophilin-dynamin complex promotes budding of clathrin-

coated vesicles during synaptic vesicle recycling. *J. Cell. Sci.* 124: 133–143, 2010.

Szejtli J. Introduction and General Overview of Cyclodextrin Chemistry. *Chem. Rev.* 98: 1743–1754, 1998.

Takahashi M, **Freed R**, **Blackmer T**, **Alford S**. Calcium influx-independent depression of transmitter release by 5-HT at lamprey spinal cord synapses. *The Journal of Physiology* 532: 323–336, 2001.

Takei K, **Mundigl O**, **Daniell L**, **De Camilli P**. The synaptic vesicle cycle: a single vesicle budding step involving clathrin and dynamin. *The Journal of Cell Biology* 133: 1237–1250, 2012.

Takei KK, **Haucke VV**, **Slepnev VV**, **Farsad KK**, **Salazar MM**, **Chen HH**, **De Camilli PP**. Generation of Coated Intermediates of Clathrin-Mediated Endocytosis on Protein-Free Liposomes. *Cell* 94: 11–11, 1998.

Taylor MJ, **Lampe M**, **Merrifield CJ**. A Feedback Loop between Dynamin and Actin Recruitment during Clathrin-Mediated Endocytosis. *PLoS Biol* 10: e1001302, 2012.

Thompson HM, **McNiven MA**. Discovery of a new 'dynasore'. *Nat Chem Biol* 2: 355–356, 2006.

Tong GG, **Jahr CEC**. Multivesicular release from excitatory synapses of cultured hippocampal neurons. *Neuron* 12: 51–59, 1994.

Vautrin J, **Barker JL**. Presynaptic quantal plasticity: Katz's original hypothesis revisited. *Synapse* 47: 184–199, 2002.

Verderio C, **Pozzi D**, **Pravettoni E**, **Inverardi F**, **Schenk U**, **Coco S**, **Proux-Gillardeaux V**, **Galli T**, **Rossetto O**, **Frassoni C**, **Matteoli M**. SNAP-25 modulation of calcium dynamics underlies differences in GABAergic and glutamatergic responsiveness to depolarization. *Neuron* 41: 599–610, 2004.

Verderio C, **Rossetto O**, **Grumelli C**, **Frassoni C**, **Montecucco C**, **Matteoli M**. Entering neurons: botulinum toxins and synaptic vesicle recycling. *EMBO Rep* 7: 995–999, 2006.

Verstreken P, **Kjaerulff O**, **Lloyd TE**, **Atkinson R**, **Zhou Y**, **Meinertzhagen IA**, **Bellen HJ**. Endophilin mutations block clathrin-mediated endocytosis but not neurotransmitter release. *Cell* 109: 101–112, 2002.

Verstreken P, **Koh T-W**, **Schulze KL**, **Zhai RG**, **Hiesinger PR**, **Zhou Y**, **Mehta SQ**, **Cao Y**, **Roos J**, **Bellen HJ**. Synaptojanin is recruited by endophilin to

promote synaptic vesicle uncoating. *Neuron* 40: 733–748, 2003.

Wagh DA, **Rasse TM**, **Asan E**, **Hofbauer A**, **Schwenkert I**, **Dürrbeck H**, **Buchner S**, **Dabauvalle M-C**, **Schmidt M**, **Qin G**, **Wichmann C**, **Kittel R**, **Sigrist SJ**, **Buchner E**. Bruchpilot, a Protein with Homology to ELKS/CAST, Is Required for Structural Integrity and Function of Synaptic Active Zones in Drosophila. *Neuron* 49: 833–844, 2006.

Wang C, **Zucker RS**. Regulation of synaptic vesicle recycling by calcium and serotonin. *Neuron* 21: 155–167, 1998.

Wang J, **Zurawski TH**, **Bodeker MO**, **Meng J**, **Boddul S**, **Aoki KR**, **Dolly JO**. Longer-acting and highly potent chimaeric inhibitors of excessive exocytosis created with domains from botulinum neurotoxin A and B. *Biochem. J.* 444: 59–67, 2012.

Wenk MRM, **Pietro P De Camilli**. Protein-lipid interactions and phosphoinositide metabolism in membrane traffic: insights from vesicle recycling in nerve terminals. *Proc Natl Acad Sci USA* 101: 8262–8269, 2004.

Wickelgren WO, **Leonard JP**, **Grimes MJ**, **Clark RD**. Ultrastructural correlates of transmitter release in presynaptic areas of lamprey reticulospinal axons. *Journal of Neuroscience* 5: 1188–1201, 1985.

Wigge P, **McMahon HT**. The amphiphysin family of proteins and their role in endocytosis at the synapse. *Trends Neurosci* 21: 339–344, 1998.

Wightman RM, **Haynes CL**. Synaptic vesicles really do kiss and run. *Nature Publishing Group* 7: 321–322, 2004.

Wu XS, **Wu LG**. Rapid Endocytosis Does Not Recycle Vesicles within the Readily Releasable Pool. *J Neurosci* 29: 11038–11042, 2009.

Wu Y, **Matsui H**, **Tomizawa K**. Amphiphysin I and regulation of synaptic vesicle endocytosis. *Acta Med. Okayama* 63: 305–323, 2009.

Xia Z, **Storm DR**. The role of calmodulin as a signal integrator for synaptic plasticity. *Nat Rev Neurosci* 6: 267–276, 2005.

Xue L, **Mei Y-A**. Synaptic vesicle recycling at the calyx of Held. *Nature Publishing Group* 32: 280–287, 2011.

Yamada H, **Padilla-Parra S**, **Park S-J**, **Itoh T**, **Chaineau M**, **Monaldi I**, **Cremona O**, **Benfenati F**, **De Camilli P**, **Coppey-Moisan M**, **Tramier M**, **Galli T**, **Takei K**. Dynamic interaction of amphiphysin with N-WASP regulates actin assembly. *Journal of Biological Chemistry* 284: 34244–34256, 2009.

Yao K, **Nagashima K**, **Miki H**. Pharmacological, Pharmacokinetic, and Clinical Properties of Benidipine Hydrochloride, a Novel, Long-Acting Calcium Channel Blocker. *J Pharmacol Sci* 100: 243–261, 2006.

Yao L, **Sakaba T**. Activity-dependent modulation of endocytosis by calmodulin at a large central synapse. *Proceedings of the National Academy of Sciences* 109: 291–296, 2012.

Yoon EJ, **Gerachshenko T**, **Spiegelberg BD**, **Alford S**, **Hamm HE**. Gbetagamma interferes with Ca2+-dependent binding of synaptotagmin to the soluble N-ethylmaleimide-sensitive factor attachment protein receptor (SNARE) complex. *Molecular Pharmacology* 72: 1210–1219, 2007a.

Yoon EJ, **Gerachshenko T**, **Spiegelberg BD**, **Alford S**, **Hamm HE**. Gbeta Interferes with Ca2+-Dependent Binding of Synaptotagmin to the Soluble N-Ethylmaleimide-Sensitive Factor Attachment Protein Receptor (SNARE) Complex. *Molecular Pharmacology* 72: 1210–1219, 2007b.

Yoshida Y, **Takei K**. Stimulation of dynamin GTPase activity by amphiphysin. *Methods in enzymology* 404: 528–537, 2005.

Zakharenko SSS, **Zablow LL**, **Siegelbaum SAS**. Altered Presynaptic Vesicle Release and Cycling during mGluR-Dependent LTD. *Neuron* 35: 12–12, 2002.

Zefirov AL, **Abdrakhmanov MM**, **Grigor'ev PN**. Kiss-and-run quantal secretion in frog nerve-muscle synapse. *Bulletin of experimental biology and medicine* 137: 107–110, 2004.

Zhang Q, **Li Y**, **Tsien RW**. The dynamic control of kiss-and-run and vesicular reuse probed with single nanoparticles. *Science* 323: 1448–1453, 2009.

Zhang X-L, **Upreti C**, **Stanton PK**. Gβγ and the C Terminus of SNAP-25 Are Necessary for Long-Term Depression of Transmitter Release. *PLoS ONE* 6: e20500, 2011.

Zhu Y, **Xu J**, **Heinemann SF**. Two Pathways of Synaptic Vesicle Retrieval Revealed by Single-Vesicle Imaging. *Neuron* 61: 397–411, 2009.

VITA

Andrew Burgess Seymour

University of Illinois at Chicago
Department of Biological Sciences
840 W. Taylor St., SEL 4263
Chicago, IL 60607
Mobile: (708) 595-2933
Work: (312) 413-3056
Email: aseymo2@uic.edu

Personal Data
Born: October 26, 1974; Grand Rapids, Michigan, USA
Citizenship: United States

Education

University of Illinois at Chicago, 2013
Chicago IL
Ph.D., Department of Biological Sciences
GPA 4.0

Loyola University Chicago, 2005
Maywood, IL
M.S., Department of Cell Biology, Neurobiology, and Anatomy
GPA 3.609

Carnegie Mellon University, 1997
Pittsburgh, PA.
B.S. Major: Psychology. Minors: French, Health Professions
College & University Honors
GPA 3.46

Professional experience

University of Illinois at Chicago 2005 – Present
Department of Biology
Research Assistant
Supervisor: Simon Alford, Ph.D.
Perform patch-clamp and intra-axonal microelectrode recordings on semi-intact lamprey spinal cord preparations
Develop and refine styryl (fluorescent) dye labeling techniques of vesicular targets in presynaptic sites in lamprey spinal cord preparations
Perform micro-dissections of lamprey spinal cord tissue
Utilize fluorescent imaging and electrophysiologic data acquisition software
Edit professional manuscripts and grants

Teaching Assistant 2005 - Present
-Comparative Vertebrate Anatomy (BioS 272)
-Animal Physiological Systems (BioS 443)
-Biology of the Brain (BioS 286)
-Cells and Organisms (BioS 100)
-Populations and Communities (BioS 101)
Supervisors: David Shomay, Ph.D., Thomas Park, Ph.D., John Leonard, Ph.D., Mike Muller, Robert Paul Malchow, Ph.D., Liang-Wei Gong, Ph.D, Alan Molunby, PhD
Designed tests and lesson plans to assess retention of content and understanding anatomical organization and physiological concepts
Organized and taught laboratory exercises, led discussions, and evaluated student presentations
Collaborated with colleagues to manage student performance
Arranged review sessions with individual students and groups

Loyola University Chicago 2000-2005
Research Assistant
Supervisor: Gwendolyn Kartje, M.D., Ph.D.
Designed functional recovery studies on rodents undergoing antibody-mediated treatment following experimental stroke surgeries
Performed stroke surgeries on rodents, including preoperative anesthesia and postoperative care
Managed and analyzed data
Prepared and edited professional manuscripts describing research pursuits
Presented findings at international and departmental meetings

Teaching Assistant Fall Semester 2002
-Gross Anatomy
Supervisors: John McNulty, Ph.D., Michael Dauzvardis, Ph.D.
Directed dissections of human cadavers in groups of medical and graduate students
Arranged review sessions with students
Organized and conducted practical exams covering human gross anatomy

Henry Ford Hospital 1999 – 2000
Department of Psychiatry
Sleep Disorders Research Center
Research Assistant
Supervisors: Thomas Roth, Ph.D., Gary Richardson, M.D.
Managed pharmaceutical studies
Conducted a study involving an artificial model of insomnia
Interviewed and recruited research participants
Collected and managed participant data
Prepared and processed laboratory samples for biochemical analyses

Children's Hospital of Philadelphia 1997- 1998
Department of Psychiatry
Research Assistant
Supervisors: Elizabeth Weller, M.D., Laura Sanchez, M.D.
Managed pharmaceutical studies
Interviewed and recruited research participants
Collected and managed participant data
Prepared and processed laboratory samples for biochemical analyses

University of Pittsburgh Medical Center 1996-1997
Western Psychiatric Institute and Clinic
Undergraduate Research Associate
Supervisors: David Rosenberg, M.D., Matcheri Keshavan, M.D.
Collected, analyzed, and managed magnetic resonance image data in studies examining structural neurodevelopmental abnormalities of pediatric patients with obsessive compulsive disorder or schizophrenia
Coauthored professional publications

Children's Hospital of Michigan Summer 1994
Wayne State University School of Medicine
Research Assistant
Supervisors: Kerry Pebbles.
Assisted in laboratory animal anesthetization, catheterization of left and right pulmonary arteries, and post-mortem dissections in cardiac and pulmonary arterial tissue studies in a clinical experiment exploring advanced angioplasty techniques

Carnegie Mellon University 1993-1994
Mellon Institute
Research Assistant
Supervisor: Elizabeth Jones, Ph.D.
Prepared yeast culture media and solutions, cleaned and maintained laboratory tools

Presentations

University of Illinois at Chicago 2005-Present
Department of Biology
Professional departmental research presentations

Loyola University Chicago 2000-2005
Department of Cell Biology, Neurobiology, and Anatomy
Professional departmental research presentations

42ND ANNUAL SOCIETY FOR NEUROSCIENCE MEETING (2012)
Poster and Abstract Title:
Dynamin Inhibition Reveals Vesicular Behavior Changes in Resting Tissue
41ST ANNUAL SOCIETY FOR NEUROSCIENCE MEETING (2011)
Poster and Abstract Title:
Dynamin's Roles in the Synaptic Vesicle Cycle at the Presynaptic Terminal
40TH ANNUAL SOCIETY FOR NEUROSCIENCE MEETING (2010)
Poster and Abstract Title:
Dynamin's Role in Kiss and Run Fusion
39TH ANNUAL SOCIETY FOR NEUROSCIENCE MEETING (2009)
Poster and Abstract Title:
Dynamin's Role in Spontaneous and Evoked Release at Presynaptic Sites in the Reticulospinal System
33RD ANNUAL SOCIETY FOR NEUROSCIENCE MEETING (2003)
Poster and Abstract Title:
Functional Recovery and Cortico-efferent Plasticity in the Adult Rat Following Sensorimotor Cortex Lesions and Delayed Nogo-A Blockade

Annual Research Day 2003
Edward J. Hines, Jr. VA Hospital
Poster and Abstract Title:
Functional Recovery and Cortico-efferent Plasticity Following Sensorimotor Cortex Lesions and Delayed Nogo-A Blockade

32ND ANNUAL SOCIETY FOR NEUROSCIENCE MEETING (2002)
Poster and Abstract Title:
Neuroanatomical Plasticity In Adult Rats Following Sensorimotor Cortex lesions and Delayed Nogo-A Blockade

Saint Albert's Day research exhibit 2002
Loyola University Medical Center
Poster and Abstract Title:
Functional Recovery in Adult Rats following Sensorimotor Cortex Lesions and Delayed Nogo-A Blockade

Meeting of the Minds Spring Semester 1997
Carnegie Mellon University
Abstract title: Attachment Style, Gender, and Relationship Type as Determinants of the Expression of Emotion

Publications

Gerachshenko T, Schwartz E, Bleckert A, Photowala H, Seymour A, Alford S. "Presynaptic G proteins as state-dependent regulators of synaptic vesicle fusion and motor behavior." Journal of Neuroscience, Volume 29, Issue 33, pp. 10221-33.

Seymour AB, Andrews EM, Tsai S-Y, Markus TM, Bollnow MR, O'Brien TE, Castro AJ, Schwab ME, Kartje GL (2005) "Delayed treatment with Nogo-A neutralization one week post-stroke results in recovery of function and corticorubral plasticity in adult rats." Journal of Cerebral Blood Flow and Metabolism, Volume 25, Issue 10, pp. 1366-1375.

Rosenberg DR, Averbach DH, O'Hearn KM, Seymour AB, Birmaher B, Sweeney JA (1997) "Oculomotor response inhibition abnormalities in pediatric obsessive compulsive disorder." Archives of General Psychiatry, Volume 54, Issue 9, pages 831-838.

Rosenberg DR, Keshavan MS, O'Hearn KM, Dick EL, Bagwell WW, Seymour AB, Montrose DM, Pierri JN, Birmaher B (1997) "Frontostriatal measurement in

treatment-naïve children with obsessive-compulsive disorder." Archives of General Psychiatry Volume 54 Issue 9, pages 824-830.

Professional Skills

Micro-dissection, patch clamp and microelectrode recordings
Vesicular imaging using fluorescent dyes in physiology experiments
Animal handling, behavioral training, and surgery
Neurohistology preparation and analysis
Experience in the following software systems: Systat, Graphpad Prism, MS Word, Excel, Powerpoint, Adobe Photoshop 7.0, Endnote 7.0, AcidPro, Final Scratch 2.0, Serato Scratch Live, Maschine 2.2, Traktor Pro 2.6
Coordinating and planning social events
Organizing fundraisers
Promoting and organizing community service endeavors

Academic Honors & Awards

Graduate Stipend — Fall 2005-present
University of Illinois at Chicago

Graduate Stipend — Fall 2001-Spring 2005
Loyola University Chicago

Psi Chi National Psychology Honor Society — 1997-Present

Undergraduate Research Fellowship — August 1996-August 1997
National Institute of Mental Health

Small Undergraduate Research Grant — 1996

Eta Chapter of Lambda Sigma Sophomore Honor Society — 1994

Dean's List — Fall 1993, Fall 1994
Carnegie Mellon University
Mellon College of Science

Dean's List — Spring 1996, Fall 1996
Carnegie Mellon University
College of Humanities and Social Sciences

N.J. & N.P. Cambell Scholarship — Spring 1995, 1996, 1997

Undergraduate Scholarship — Fall 1993-94,
Carnegie Mellon University — Fall 1995, 1997

International Studies Association Scholarship — Fall 1993

National Office Products Association (NOPA) Scholarship — Fall 1993

Extracurricular Activities

Training in Hapkido, a Korean martial art — 2002-present
Grandmaster K.S. Hyun's Hapkido School, Chicago, IL
Awarded black belt, second dan — 2012
Promoted to assistant instructor — 2009

The Neurotransmitter — 2003-2005
Authored column in biannual publication from the Neuroscience and Aging Institute (NSAI) at Loyola University Medical Center

Graduate Student Council President — 2002-2003
Loyola University Medical Center

Graduate Student Council representative — 2001-2002
Loyola University Medical Center

Secretary for AIDS Partnership Michigan (APM) — 1998-2000
Prepared information packets concerning HIV status and health care, administered consent forms, and coordinated with HIV testing counselors.

Buddy Program, ActionAIDS — 1998-2000
Philadelphia, PA
-Met with a person living with HIV/AIDS on a regular basis as a means of providing unstructured social support
-Attended regular training meetings with ActionAIDS to maintain ethical and safety standards

Surgery Workshop — 1998
Philadelphia College of Osteopathic Medicine
-Assisted intersupine grafting of small intestine to infrarenal aorta.

Lambda Sigma Sophomore Honor Society — 1994-1995
Carnegie Mellon University

-Service Committee Chairperson

Diversity Roundtable Discussion Leader 1993-1994
Carnegie Mellon University
-Organized and led group meetings on topics of race, gender, and religious relations on campus and in surrounding community.